Journal of Marine Research, 52, 55–81, 1994

Water-mass distributions in the western South Atlantic; A section from South Georgia Island (54S) northward across the equator

by Mizuki Tsuchiya[1], Lynne D. Talley[1] and Michael S. McCartney[2]

ABSTRACT

A long CTD/hydrographic section with closely spaced stations was made in February–April 1989 in the western Atlantic Ocean between 0°40′N and South Georgia (54S) along a nominal longitude of 25W. Vertical sections of various properties from CTD and discrete water-sample measurements are presented and discussed in terms of the large-scale circulation of the South Atlantic Ocean.

One of the most important results is the identification of various deep-reaching fronts in relation to the large-scale circulation and the distribution of mode waters. Five major fronts are clearly defined in the thermal and salinity fields. These are the Polar (49.5S), Subantarctic (45S), Subtropical (41–42S), Brazil Current (35S) Fronts, and an additional front at 20–22S. The first three are associated with strong baroclinic shear. The Brazil Current Front is a boundary between the denser and lighter types of the Subantarctic Mode Water (SAMW), and the 20–22S front marks the boundary between the anticyclonic subtropical and cyclonic subequatorial gyres. The latter front coincides with the northern terminus of the high-oxygen tongue of the Antarctic Intermediate Water (AAIW) and also with the abrupt shift in density of the high-silica tongue originating in the Upper Circumpolar Water and extending northward. Two pycnostads with temperatures 20–24°C are observed between 10S and 25S with the denser one in the subtropical and the other lighter one in the subequatorial gyre. A weak thermostad centered at 4°C occurs in the AAIW between the Subtropical Front and the Subantarctic Front and shows characteristics similar to the densest variety of the SAMW.

Another significant result is a detailed description of the complex structure of the deep and bottom waters. The North Atlantic Deep Water (NADW) north of 25S contains two vertical maxima of oxygen (at 2000 m and 3700 m near the equator) separated by intervening low-oxygen water with more influence from the Circumpolar Water. Each maximum is associated with a maximum of salinity and minima of nutrients. The deeper salinity maximum is only weakly defined and is limited to north of 18S, appearing more as vertically uniform salinity. South of 25S the NADW shows only a single maximum of salinity, a single maximum of oxygen, and a single minimum of each nutrient, all lying close together. The salinity maximum south of 25S and the deeper oxygen/salinity maximum north of 11S are derived from the same source waters. The less dense NADW containing the shallower extrema of characteristics turns to the east at lower latitudes and does not reach the region south of 25S. The

1. Scripps Institution of Oceanography, University of California, San Diego, La Jolla, California, 92093-0230, U.S.A.

2. Woods Hole Oceanographic Institution, Woods Hole, Massachusetts, 02543, U.S.A.

southward spreading of the NADW is interrupted by domains of intensified circumpolar characteristics. This structure is closely related to the basin-scale gyre circulation pattern.

The Weddell Sea Deep Water is the densest water we observed and forms a relatively homogeneous layer at the bottom of the Georgia and Argentine Basins. The bottom layer of the Brazil Basin is occupied by the vertically and laterally homogeneous Lower Circumpolar Water.

1. Introduction

A long CTD/hydrographic section with closely spaced stations was occupied across the equator between Iceland (63N) and South Georgia (54S) to investigate the mid-ocean circulation at all depths of the Atlantic Ocean and to augment global baseline data for the study of the large-scale ocean circulation. The field work was divided into two parts. The northern half of the transect was occupied by R/V *Oceanus* in July–August 1988, and the southern half by R/V *Melville* in February–April 1989 with some overlapping stations near the equator. In a previous paper (Tsuchiya *et al.,* 1992), the data from the northern half have been illustrated and interpreted in terms of the large-scale ocean circulation. The present paper displays the full-depth vertical sections of properties observed along the southern half of the transect with a discussion of some features of interest in the distributions.

The *Melville's* 1989 South Atlantic cruise (Hydros 3 and 4) was coordinated and integrated with the South Atlantic Ventilation Experiment (SAVE).[3] The locations of the stations are shown in Figure 1. The southern half of the transect (Stas. 237–278) was occupied on 1–17 February during Hydros 3. The station intervals were 56 km except near South Georgia, where closer spacing was chosen over the sharp bottom slope. The northern half of the transect (Stas. 314–373) was occupied on 21 March–8 April during Hydros 4. The station spacing for this portion of the transect was 37 km north of 1S, 56 km between 1S and 4S, and 65 km elsewhere. Except near its northern end, where it reaches the Mid-Atlantic Ridge, the transect lies in the western basin of the South Atlantic.

The field measurements were carried out in essentially the same manner as on the North Atlantic cruise in the previous year except that a 36-bottle rosette sampler was used on the *Melville.* The accuracies and precisions of the CTD and discrete measurements are the same as or better than those reported for the North Atlantic cruise (Tsuchiya *et al.,* 1992). Tabulated data have been published in data reports (Scripps Institution of Oceanography, 1992a,b).

Vertical sections of potential temperature, salinity, and potential density (σ_θ and σ_2/σ_4), based on the CTD data, are presented in Figures 2–4, and those of dissolved oxygen, silica, phosphate, and nitrate, based on the bottle data, are presented in Figures 5–8. The vertical exaggeration of the full-depth sections is 500 while that for

3. Therefore, Hydros 3 and 4 are also referred to as SAVE 5 and 6, respectively. Consecutive station numbers are used throughout all SAVE cruises.

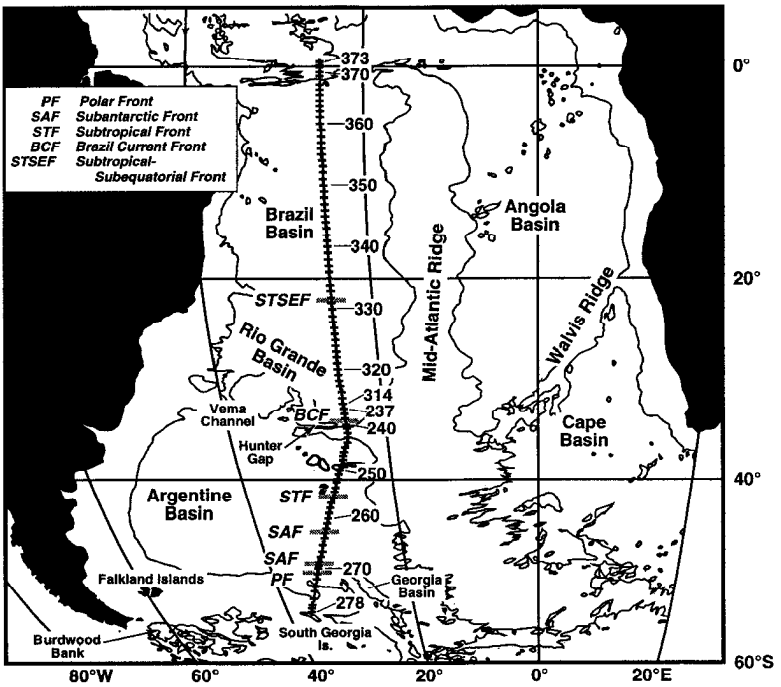

Figure 1. Station locations of the long CTD/hydrographic section at a nominal longitude of 25W occupied by R/V *Melville* on Hydros 3/4, February–April 1989, with the 4000 m isobath. The section was broken into two legs. The first leg (Hydros 3) ran from 32°30′S, 25° 0′W (Sta. 237) southwestward to 53°57′S, 36°24′W (Sta. 278) on the north coast of South Georgia and took 16 days to complete. The second leg (Hydros 4) ran from 32° 0′S, 25° 0′W (Sta. 314) northward to 0°40′N, 25° 0′W (Sta. 373) and took 18 days to complete. Note that the time interval between Sta. 237 and Sta. 314 was 48 days. The positions of major water-mass fronts observed along the section and referred to in the text are also indicated.

the top 1.5 km repeated in the upper panel is increased to 1250. All density-anomaly values (σ_θ, σ_2, etc) quoted in this paper are calculated according to the International Equation of State (EOS80), with the units being kg m^{-3}.

2. Fronts and near-surface waters

Of particular importance to our discussion are the various permanent fronts (Fig. 1), most of which extend over much of the water column depth. Peterson and Stramma (1991) present a useful updated version of these structures for the South Atlantic. Our discussion is primarily in terms of property distributions on isopycnals and in water mass core layers, rather than in terms of strong baroclinic currents. Using the properties as a guide, we identify the Polar Front at 49°30′S, the Subantarctic Front at 45S, the Subtropical Front at 41S, the Brazil Current Front at 34–36S, and the front between the subtropical anticyclonic and subequatorial

cyclonic circulations at 20–21S. The Subantarctic Front was complicated on our section by a meander or eddy so that there is a second crossing of the front at 48S; frequent meandering of the front a little farther west was documented by Whitworth *et al.* (1991). We extend Peterson and Stramma's Brazil Current Front at least as far eastward as 25W, where it appears at 34–36S. It may even continue eastward across the Mid-Atlantic Ridge, where it is apparent in another SAVE section (Gordon *et al.,* 1992, who identify it as the Benguela/South Atlantic Current Front).

The warm, saline tropical water is best developed at 0–100 m just above the pycnocline between 13S and 25S, and its highest salinity (~37.27 psu) occurs at the sea surface near 21S. This saline water extends both equatorward and poleward. The equatorward extension is seen as a tongue with its axis along $\sigma_\theta \sim 24.5$ (depth ~80 m) in the middle of the sharp pycnocline. Along the axis, maximum salinity decreases to the north reaching a lateral minimum near 2S. Farther north, maximum salinity increases across the equator toward the north end of the section (0°40'N).

The poleward extension of the high-salinity water can be traced in the surface layer as far as the Brazil Current Front, where the surface salinity is reduced to ~35.5 psu. The northward-rising isopycnals in the top 1 km north of ~30S indicate that the major part of the high-salinity water remains in the westward-flowing limb of the subtropical gyre, i.e., the South Equatorial Current.

Poleward of the Brazil Current Front, a subsurface salinity maximum is found at ~100 m just beneath the pycnocline. This water is denser ($\sigma_\theta = 26.5$–26.6) and less saline (<35.5 psu) than the high-salinity water to the north and appears to be advected from the west by the South Atlantic Current (Stramma and Peterson, 1990). The maximum salinity is sharply reduced near 41–42S from 35.4 to 34.7 psu. A similarly strong salinity gradient is found also at the sea surface. Following the terminology of Peterson and Stramma (1991), we identify it as the Subtropical Front. It is another of the eastward extensions of the Brazil Current (Roden, 1986). The Subtropical Front is accompanied by strong temperature and density gradients. Below 1500 m, the gradients are weaker but extend throughout the water column, and similar slopes of isopleths are clear in the salinity, oxygen, and nutrient sections below 2000 m.

The salinity maximum extends farther poleward across the Subtropical Front, but becomes still denser ($\sigma_\theta = 26.8$–26.9) and weaker, breaking up into isolated cores. At 45S there is again a fairly strong horizontal salinity gradient accompanied by a similarly strong temperature gradient. The isopycnals below the pycnocline rise steeply southward at the same latitude, probably reflecting the eastward flow of the Falkland Current extension. All of these features are identified with the Subantarctic Front. The last trace of the saline subsurface water is found immediately north of the Polar Front, which coincides with the northern limit of the well-defined temperature minimum (120–150 m) embedded between the warm summer surface water and the temperature maximum at 400–500 m.

Figures 2 through 8 follow

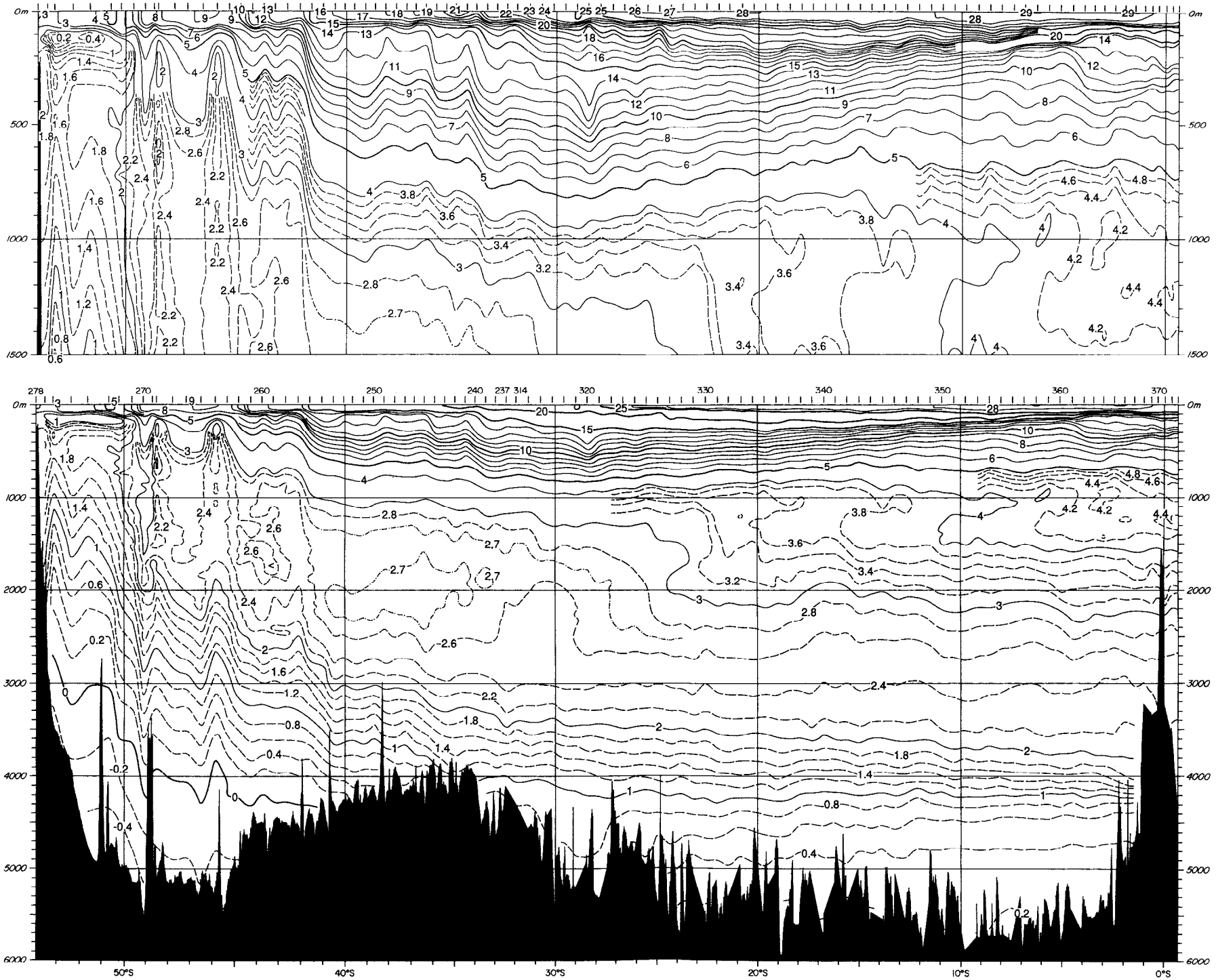

Figure 2. Vertical section of potential temperature (°C) from Hydros 3/4, February–April 1989, based on CTD data. The vertical exaggeration is 1250 in the upper panel and 500 in the lower panel.

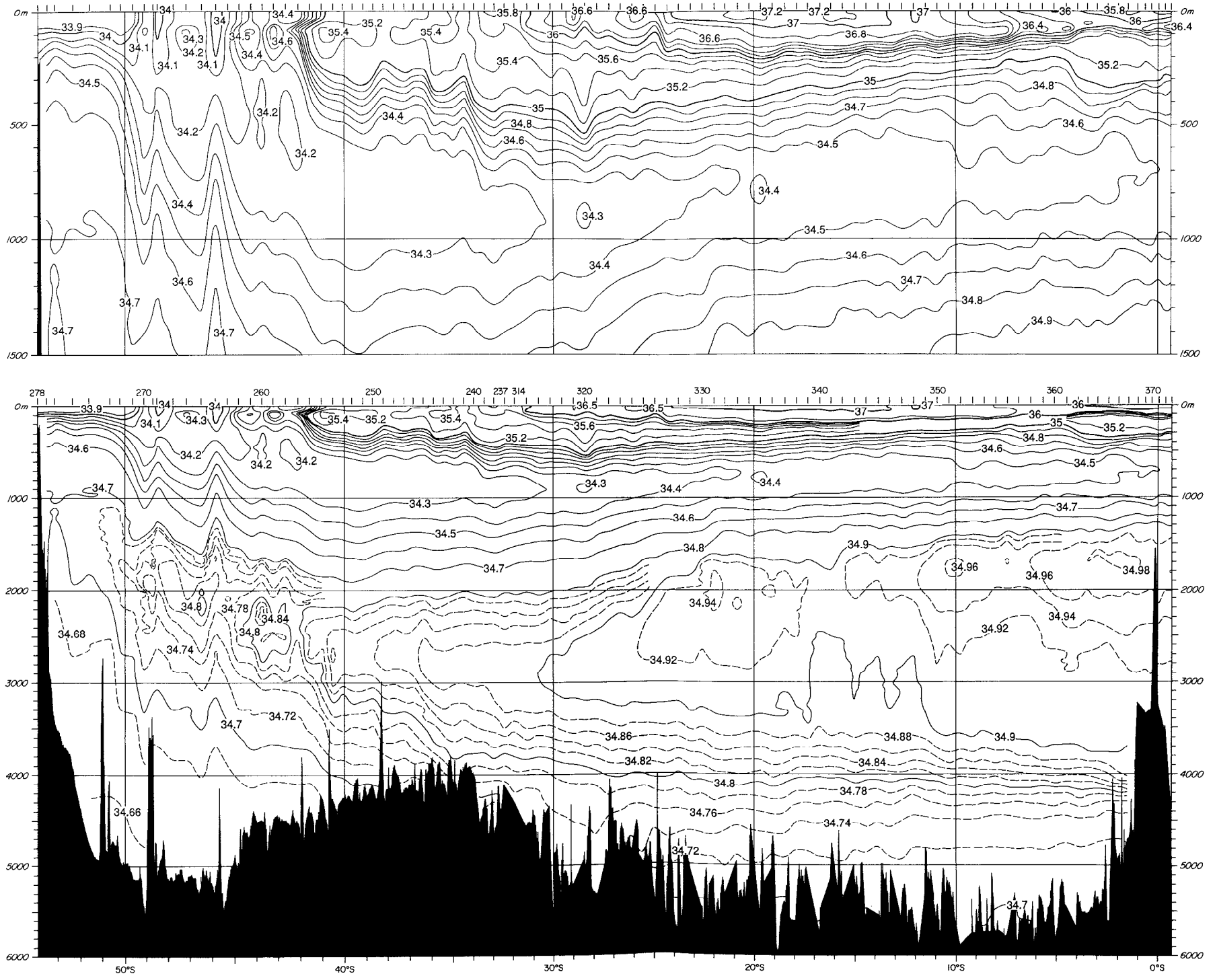

Figure 3. Vertical section of salinity (psu) from Hydros 3/4, February–April 1989, based on CTD data.

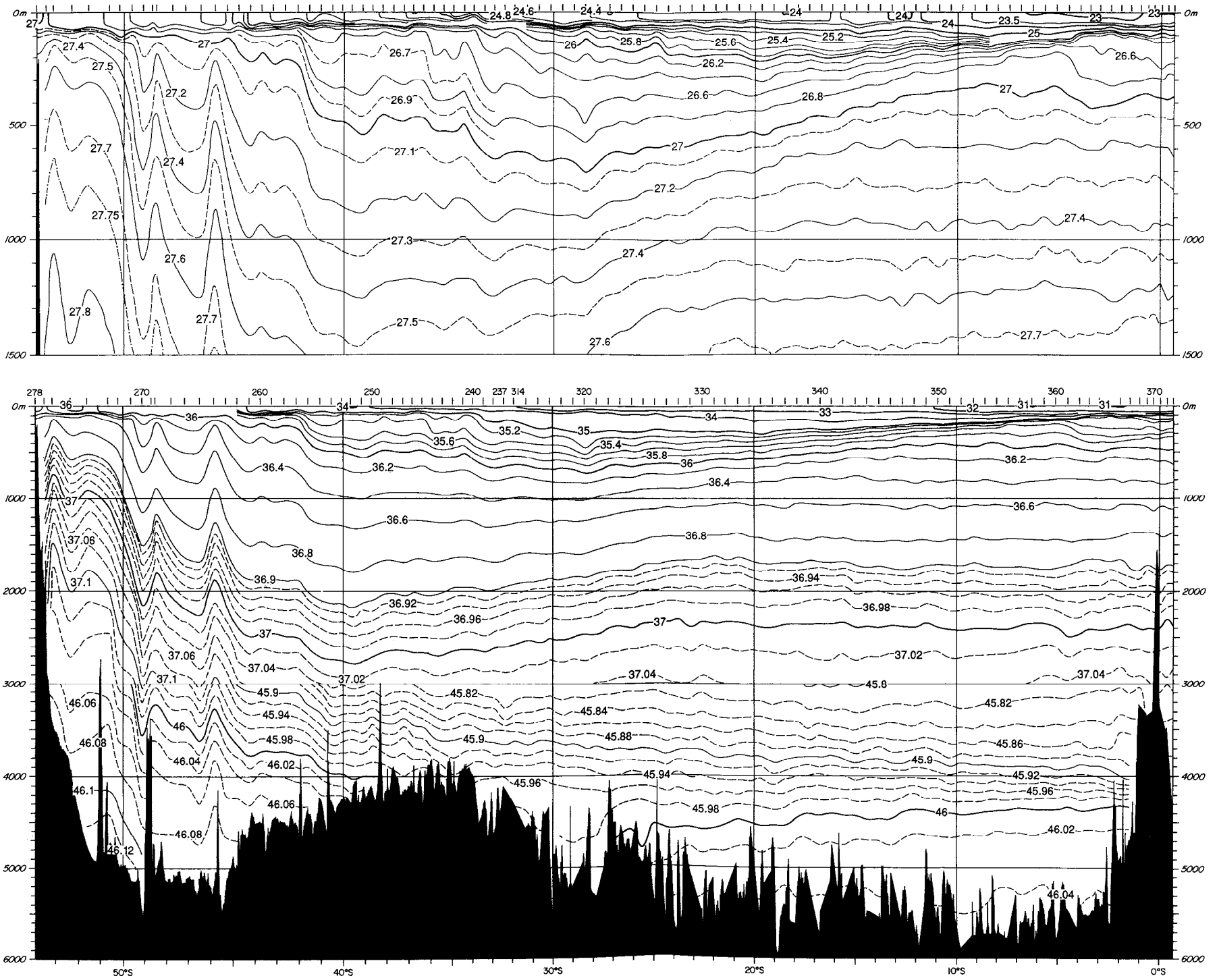

Figure 4. Vertical section of potential density (kg m^{-3}) from Hydros 3/4, February–April 1989, based on CTD data. The upper panel shows σ_θ, while the lower panel shows σ_2 for 0–3000 m and σ_4 for depths greater than 3000 m.

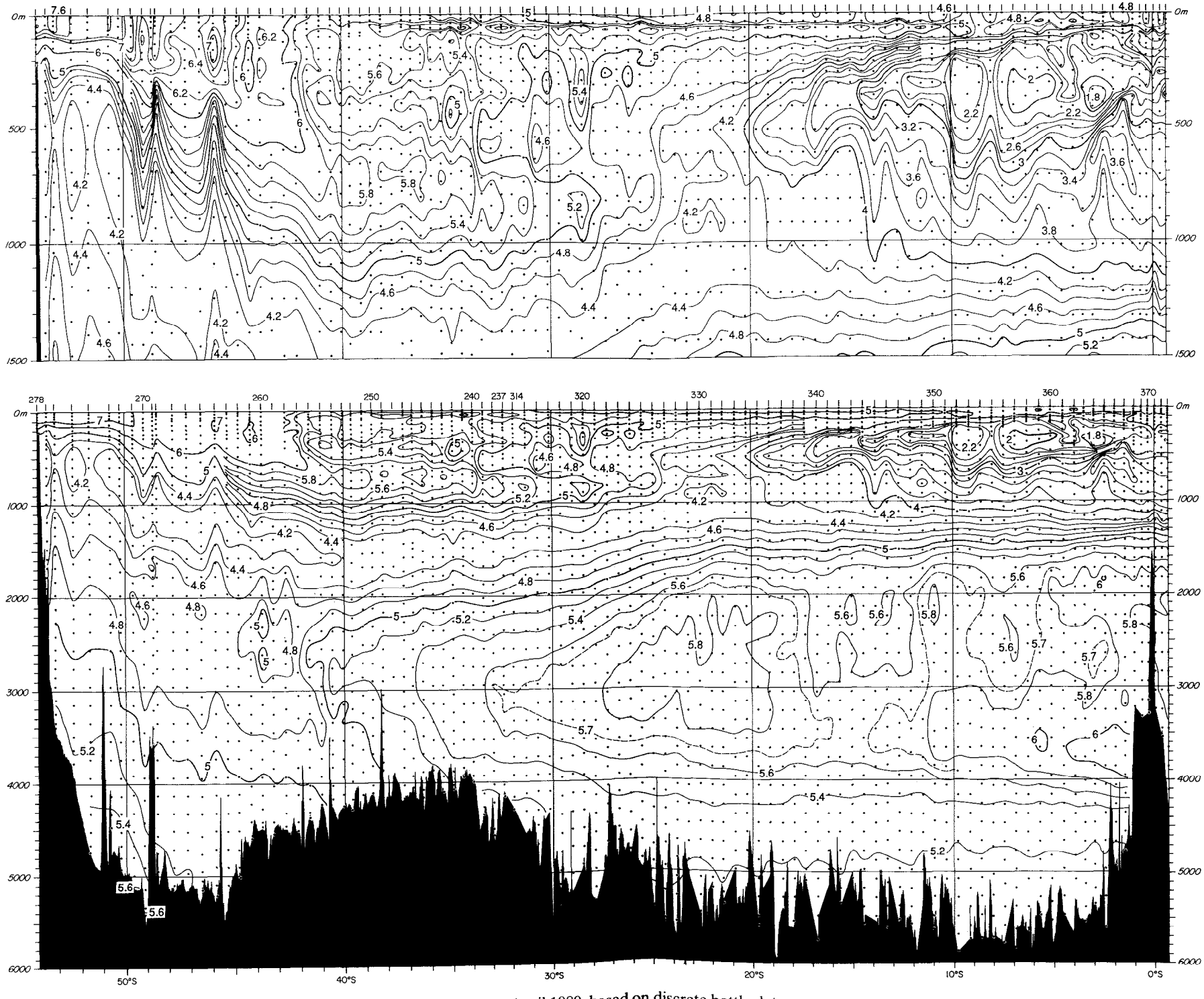

Figure 5. Vertical section of oxygen (ml l^{-1}) from Hydros 3/4, February–April 1989, based on discrete bottle data.

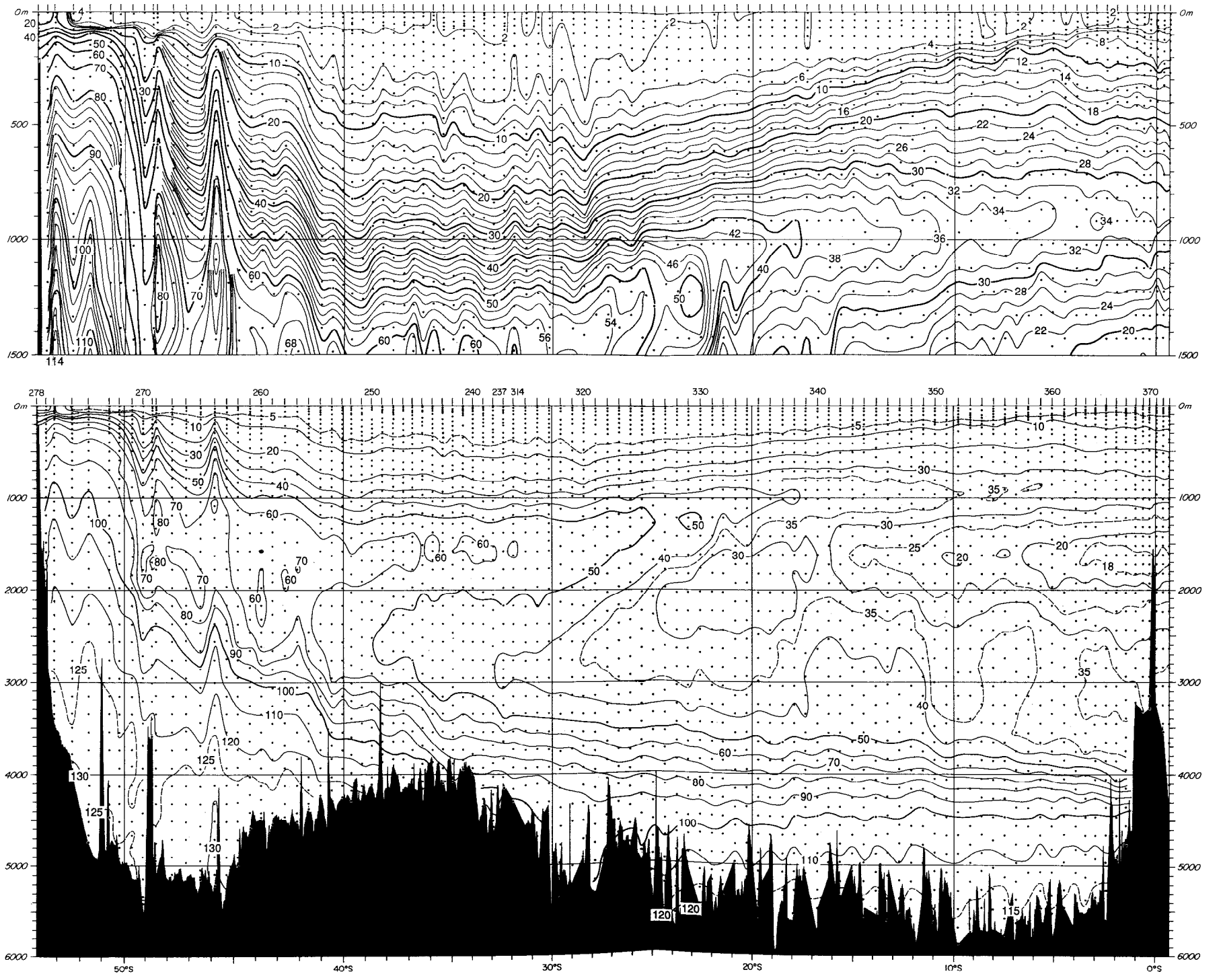

Figure 6. Vertical section of silica (μmol kg^{-1}) from Hydros 3/4, February–April 1989, based on discrete bottle data.

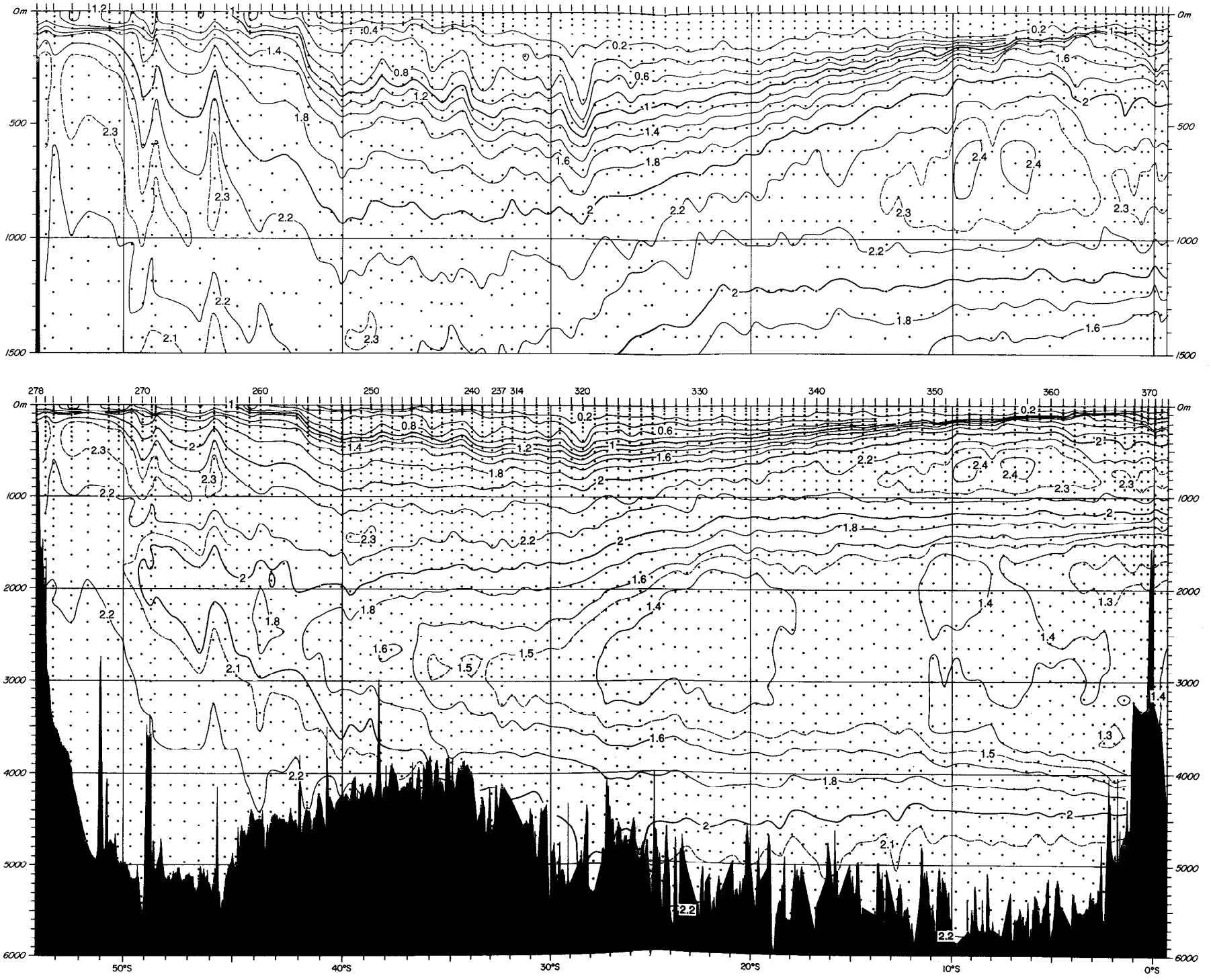

Figure 7. Vertical section of phosphate (μmol kg^{-1}) from Hydros 3/4, February–April 1989, based on discrete bottle data.

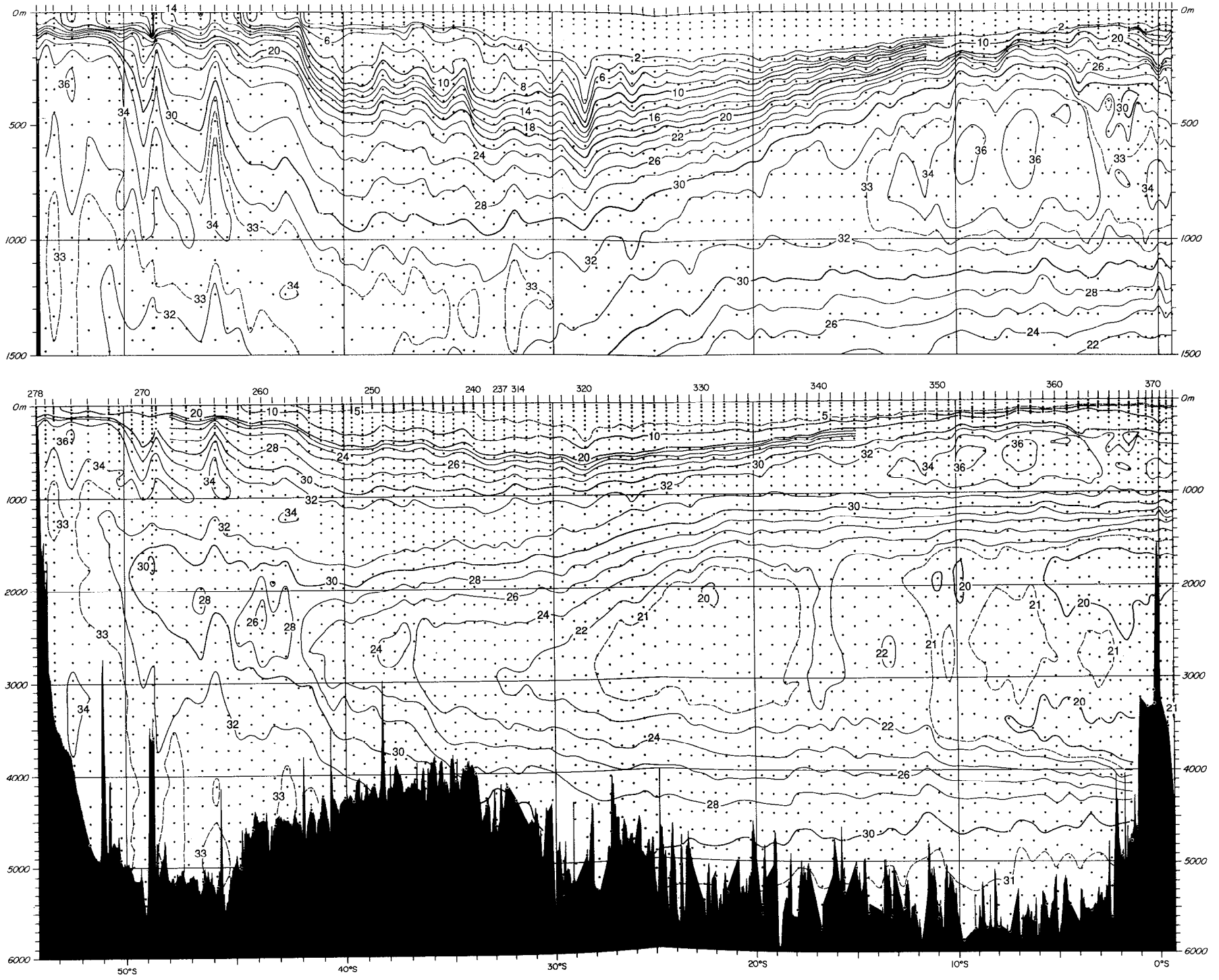

Figure 8. Vertical section of nitrate (μmol kg^{-1}) from Hydros 3/4, February–April 1989, based on discrete bottle data.

Between 24°30′S and 11°30′S, where the high salinity tropical water is best developed, there is a pycnostad (thermostad) at 25.0–25.8 σ_θ (20–24°C) in the upper 200 m. The southern edge of the pycnostad coincides with steeply-sloping isopycnals, indicating relatively strong eastward shear, although little eastward transport is associated with this shallow flow. Between this front and 19–20S, the pycnostad properties are approximately 25.6 σ_θ, 21°C, and 36.5 psu. North of 19–20S, the properties shift abruptly to 25.4 σ_θ, 22.5°C, and 36.7 psu.

The South Atlantic anticyclonic gyre has two centers near 22S and 32S just off the coast of South America (Tsuchiya, 1985). The 25.6 σ_θ mode water is associated with the northern gyre. The 25.4 σ_θ mode water is apparently on the southern side of the cyclonic subequatorial gyre. Associated with the southern gyre is the Subantarctic Mode Water (SAMW), discussed in the next section. A full discussion of these South Atlantic mode waters is beyond the scope of this paper but is being pursued.

3. Subantarctic Mode Water

The SAMW is recognizable as a strong pycnostad (Figs. 4 and 9) from the Subtropical Front (42S) as far north as 20S, where it underlies the shallow 25.6 σ_θ mode water. The northern limit ($\sim$20S) of the pycnostad coincides nearly with the boundary between the anticyclonic subtropical gyre and the cyclonic subequatorial gyre, as will be discussed below (Sections 4 and 5) and as is apparent in Reid's (1989) adjusted steric heights at 250 and 500 dbar. South of 36S, where the pycnostad is thick ($\sim$200 m), well-developed (low potential vorticity), and of nearly uniform properties, the pycnostad temperature, salinity, and potential density are 11.6°C, 35.1 psu, and 26.72 σ_θ. At 36S, the pycnostad properties shift abruptly to 13–13.5°C, 35.2–35.4 psu and 26.5–26.6 σ_θ. This 26.6 σ_θ SAMW is the mode water associated with the southern of the two anticyclonic gyres of the subtropical South Atlantic mentioned just above.

The boundary between the denser and lighter types of the SAMW at 36S along the 25W section coincides with strong isopycnal slopes, indicating a front. A similar front is found at 33–34S on the SAVE section lying to the east at about 10W (Gordon *et al.*, 1992). We suggest that the boundaries on both sections are eastward extensions of the Brazil Current Front (Peterson and Stramma, 1991), which has been observed to separate the two types of SAMW farther west at 42W (Roden, 1986). Other strong isopycnal slopes are observed along 25W, at 34S and 38.5S, but do not coincide with property boundaries in the SAMW. This strong zonation with a horizontal scale of 200–250 km is characteristic of the poleward side of the subtropical gyres, in which the general flow is eastward.

Although not clearly seen on the vertical section, a vertical maximum of oxygen in the SAMW is apparent in the CTD profiles south of 31S (Figs. 9b and 9d). The maximum is suggestive of the convective origin of the pycnostads. North of 31S, the layer identified as the SAMW separates overlying northward-deepening isopycnals

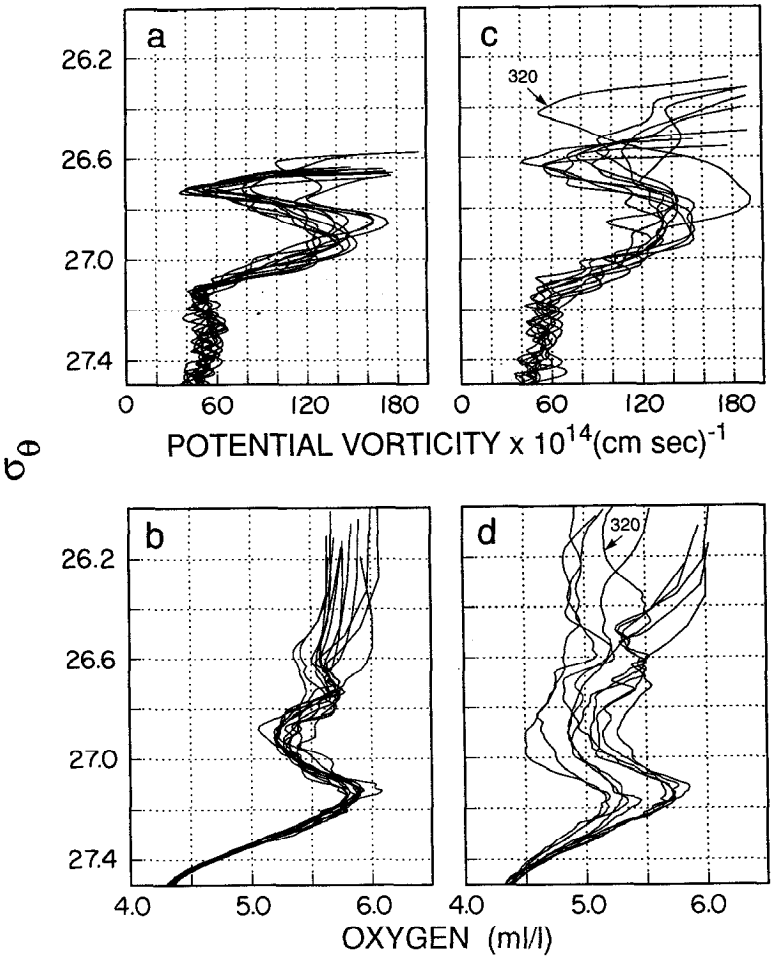

Figure 9. (a) Potential vorticity (10^{-14} $cm^{-1}s^{-1}$) and (b) oxygen (ml l^{-1}) as a function of potential density σ_θ from CTD profiles at Stas 256–245 (southern SAMW along the 25W section, between 42S and 36S). (c) Potential vorticity (10^{-14} $cm^{-1}s^{-1}$) and (d) oxygen (ml l^{-1}) from CTD profiles at Stas 244–238, 314–315 (northern SAMW along the 25W section, between 36S and 31S) and Sta. 320 (28°29'S). Potential vorticity (f/ρ) ($\partial\rho/\partial z$) was calculated from the Brunt-Vaisala frequency; the contribution from relative vorticity was not included.

from underlying northward-shoaling isopycnals. This wedging of the thermocline in the equatorward side of subtropical gyres is a global feature of mode water distributions and is reflected by a poleward shift with depth of the subtropical gyre center. There is no oxygen maximum associated with this SAMW regime, and the potential vorticity is nearly vertically uniform with a slight minimum rather than a pronounced minimum. This pattern ceases abruptly at 20S, with all isopycnals

shoaling to the north of there and no layer of vertically-uniform potential vorticity. A strong eddy at Sta. 320 (28S) interrupts this pattern, with a thick pycnostad of the SAMW at 26.42 σ_θ (14.6°C); it is discussed below.

McCartney (1977, 1982) showed that the SAMW in the South Atlantic is formed by winter convection at about 40S, north of the Subtropical Front and, using potential vorticity as its tracer, inferred anticyclonic circulation of the SAMW in the South Atlantic subtropical gyre. He found its distribution to be limited to a relatively small area west of 20W and south of 25S. Depending on the definition of the SAMW, the new data show the SAMW region to be more restricted along 25W, to the south of 31S, where there is a well-defined potential-vorticity minimum, or less restricted, to the south of 20S, where the potential vorticity is either vertically uniform or has a slight minimum. Examination of the other SAVE CTD data (in progress) shows that the SAMW is best developed along the 25W section, but that there is weak, less uniform SAMW as far east as 5W at 30S.

An anticyclonic eddy is found at 28.5S (Sta. 320). Its SAMW is much better developed, with much lower potential vorticity, than any other SAMW on the section (Fig. 9), and is marked by a vertical and lateral maximum of oxygen (>5.4 ml l^{-1}). Anomalous spreading of isotherms is centered at 15°C, isohalines at 35.5 psu, and isopycnals at 26.4 σ_θ. The upward spread extends to the bottom of the surface mixed layer and the downward spread to 800 m. Although not apparent in the vertical sections, there is also a pycnostad shallower than the SAMW, centered at 26.1 σ_θ and extending one station on either side of Sta. 320. An isolated bubble of the Antarctic Intermediate Water (AAIW) (Section 4) is found below the most obvious isopycnal deflections. This station is located at the deepest point of isopycnals between 26.4 and 27.1 σ_θ. The nutrient sections exhibit similar patterns but isopleths spread only downward. The SAMW at this station is 14.6°C, 35.48 psu, 26.42 σ_θ. It matches SAMW found within the loop of the Brazil Current at 38S by Gordon (1981). Other characteristics also suggest that this anomaly originated to the southwest, hence in the Brazil Current region, rather than in the Agulhas retroflection, where numerous anticyclonic eddies are generated and migrate westward (Gordon and Haxby, 1990). Geostrophic velocity calculations relative to 1000 dbar (Fig. 10) indicate that the anticyclone is subsurface intensified, and its maximum rotational speed is at 300 m (15°C, 26.4 σ_θ). Its geostrophic velocity signature, of a nearly symmetric eddy, encompasses a group of five stations centered at Sta. 320. The presence of anticyclonic eddies in subtropical gyres is puzzling; Brundage and Dugan (1986) document a number of North Atlantic sitings involving anomalous 18°C Water in the Sargasso Sea. McCartney and Woodgate-Jones (1991) report one of Agulhas origin in the eastern subtropical Atlantic. The eddy we observe sits between the latitudes of the two anticyclones of the Brazil Current (Tsuchiya, 1985), which we assume extend as far as 25W based on this new section.

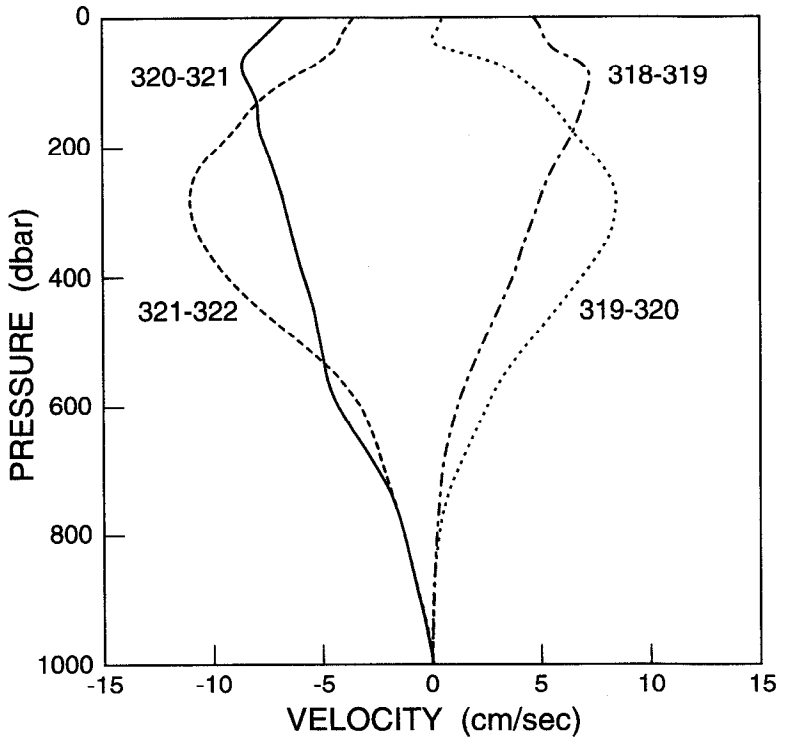

Figure 10. Geostrophic velocity (cm s^{-1}) relative to 1000 dbar for stations bracketing the anticyclonic eddy at Sta 320 (28°29'S).

4. Antarctic Intermediate Water

The AAIW is the most prominent feature in the upper 1.5 km of the salinity section. It is recognized as a low-salinity tongue at a depth of about 300 m near the Subantarctic Front (45S), descending northward to 900 m at 30S in the vicinity of the subtropical gyre center, and rising again to 700 m at the equator. At the core of the salinity minimum (Fig. 11), potential temperature, density, and salinity all increase equatorward. South of 45S are found scattered salinity minima in the upper 300 m, which may be due to the meandering Subantarctic Front and hence broken Subantarctic Zone.

In the Subantarctic Zone between the Subantarctic Front and the Subtropical Front (41S), the AAIW forms a weak pycnostad and thermostad at the base of the pycnocline; the salinity minimum is centered at about 27.15 σ_θ, 4°C and 34.2 psu, with two colder observations near 3.5°C. The weak potential-vorticity minimum is evident in Figure 9a and is associated with a pronounced oxygen maximum. The potential-vorticity minimum was previously observed at 42W by Roden (1989). This is the newest AAIW on the section and can be traced back to the Subantarctic Zone north of the Subantarctic Front just east of Drake Passage (e.g., Peterson and Whitworth,

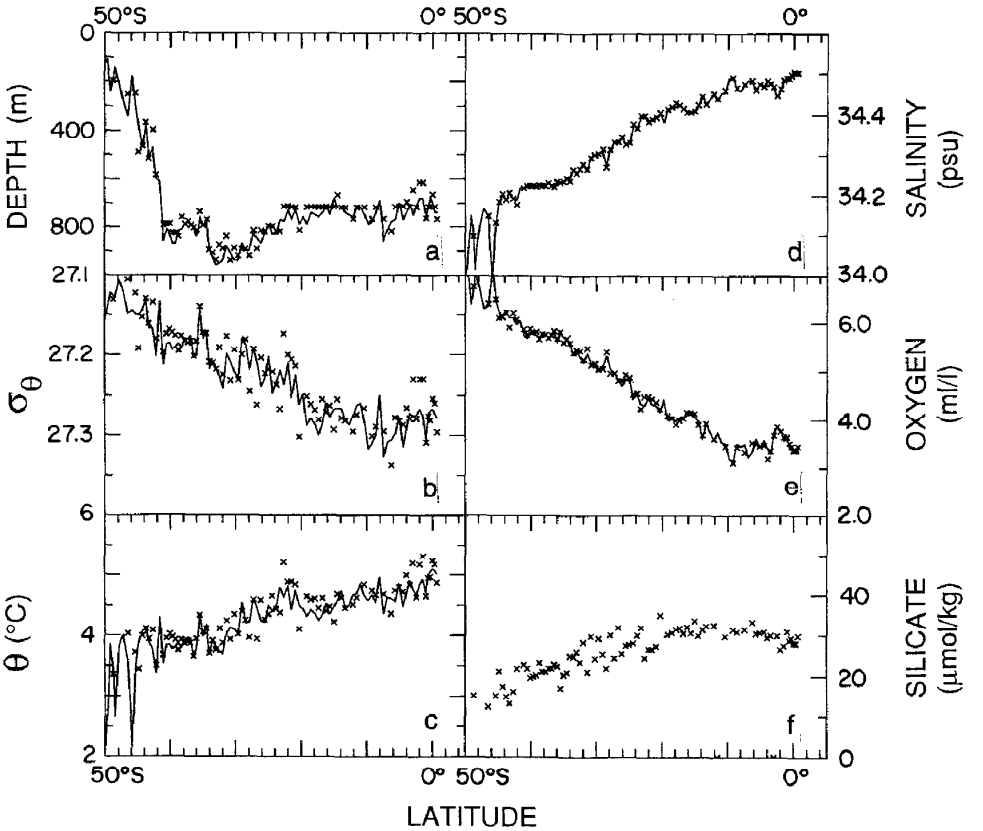

Figure 11. Properties at the absolute salinity minimum along the Hydros 25W section in the density range 27.1–27.4 σ_θ. North of the Subantarctic Front at 45S, the minimum is identified as Antarctic Intermediate Water. (a) Depth (m), (b) potential density σ_θ, (c) potential temperature (°C), (d) salinity (psu), (e) oxygen (ml l^{-1}), and (f) silica (μmol kg^{-1}). The solid curve is CTD data and the x's are bottle data. No vertical interpolation was used for the latter.

1989). These characteristics are similar to those of the densest variety of SAMW formed in late winter just east of Drake Passage: McCartney (1977) and Piola and Gordon (1989) reported SAMW at about 4.2°C, 34.16 psu near Burdwood Bank in 1934 and 1980 respectively, suggesting remarkable climatic stability for the SAMW. The issue of whether this densest SAMW is the direct precursor of AAIW (McCartney, 1977) or whether substantial input across the Subantarctic Front is necessary (Piola and Gordon, 1989) is being addressed separately. The argument in favor of the former is that the densest SAMW in late winter is fresher than the underlying AAIW, and with the SAMW's high-oxygen content and low salinity and with vertical mixing from the convecting SAMW, the AAIW can be renewed by the SAMW rather than by fluxes of oxygen and freshwater across the Subantarctic Front.

Between the Subtropical Front and the Brazil Current Front (34S) the AAIW has uniform salinity and potential temperature near 34.22 psu and 4°C. At 34S there is a transition at which the core deepens 100 m toward the north and salinity and potential temperature begin to rise. This transition is one means of identifying this front as the eastward extension of the Brazil Current.

The high-oxygen tongue of the AAIW is at a slightly lower density (σ_θ = 27.15–27.20) than the salinity minimum. Unlike the salinity minimum, the oxygen maximum terminates at 21S, which is the boundary between the subtropical gyre and the cyclonic subequatorial gyre at this depth (Reid, 1989). A few weak oxygen maxima at a somewhat higher density (27.3 σ_θ) are found between 21S and 11S, but are not revealed by the vertical section (Fig. 5). The oxygen content in the tongue decreases from >6 ml l^{-1} near its origin to 4.4 ml l^{-1} near 21S. North of 21S the deeper portion of the low-oxygen equatorial water dominates the entire depth range of the AAIW, except for a small core of high oxygen (>3.6 ml l^{-1}) at 600–700 m ($\sigma_\theta \sim 27.2$) between 1S and 3S, centered at 2°30′S.

The relatively higher oxygen between 1S and 3S is accompanied by low salinity. This is further illustrated with salinity at 27.2 σ_θ (Fig. 12) in which the full extent and coherence of the tongue is evident, with its source at the western boundary, and extension nearly to the eastern boundary. A separate study of AAIW using these datasets (Suga and Talley, 1994) shows a very weak tongue of low salinity just north of the equator on a slightly deeper isopycnal, suggesting eastward flow there. Between the isopycnic salinity minima, salinity is essentially uniform on isopycnals through the AAIW. We have not yet determined whether the equatorial flow is westward or eastward. Cores of high phosphate and nitrate near the equator at 700–800 m ($\sigma_\theta \sim 27.3$) in the vertical sections suggest that the equatorial flow extends down to at least the density of these maxima.

The termination of the high-oxygen tongue of the AAIW near 21S is related to the basin-scale circulation pattern of the AAIW. The AAIW associated with the high oxygen south of 21S is newer and circulating anticyclonically in the subtropical gyre (Reid, 1989; Gordon *et al.,* 1992; Rintoul, 1991; Zemba, 1991). The lower oxygen north of 21S is the southern westward-flowing limb of the cyclonic subequatorial gyre in which the AAIW was advected eastward near the equator, as described in the previous paragraph, and is returning westward farther south. In this gyre, the AAIW oxygen is severely reduced by consumption. Figure 12 indicates that there is a region of high salinity in the eastern part of this cyclonic gyre, which is only weakly evident in Reid's (1989) salinity map at 27.3 σ_θ and which coincides with the region of very low oxygen in his oxygen map for the same σ_θ. The high salinity is unlikely to come from the North Atlantic because the low-salinity AAIW just south of the equator extends almost all the way to the eastern boundary. There is also isolated high salinity (>34.575 psu) pressed against the African coast within the gyre. Therefore, there must be vertical mixing in this region, as noted by Gordon and Bosley (1991).

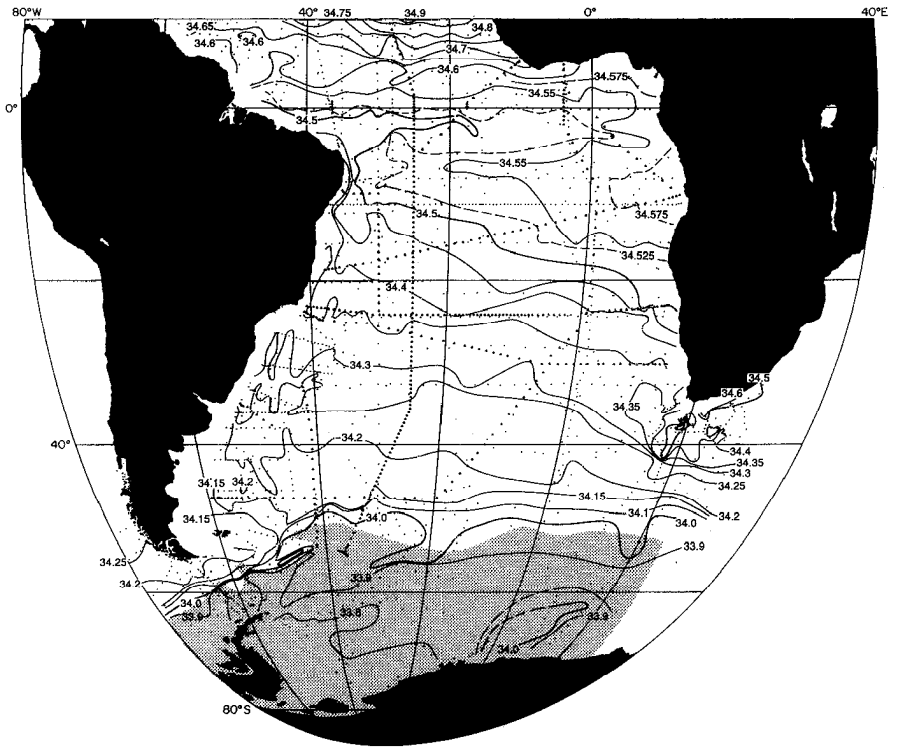

Figure 12. Salinity (psu) on the 27.2 σ_θ isopycnal, which intersects the salinity minimum of the Antarctic Intermediate Water between 25S and 40S at 25W. Both CTD (triangles) and bottle (dots) data were used. The shaded region is where the isopycnal shoals to less than 100 m.

No vertical extrema of nutrients occur in the depth range of the AAIW from its origin northward to ~21S, where its high-oxygen tongue terminates. Farther north, however, the phosphate and nitrate maxima, which lie below the intense oxygen minimum of the equatorial water, are roughly coincident with the salinity minimum of the AAIW. In the same region north of 21S, silica also shows a vertical maximum at a somewhat greater density (σ_θ ~ 27.4). These nutrient maxima north of 21S should not be regarded as the northward extensions of those found farther south at higher densities below the AAIW, where they characterize the Upper Circumpolar Water (UCPW) (Section 5), although they do appear as continuous tongues on the vertical sections. The phosphate and nitrate maxima are clearly associated with the oxygen minimum produced by excess consumption in the cyclonic gyre, whereas silica is not much affected by fallout from the euphotic zone. Since silica increases downward through the AAIW into the UCPW (Fig. 6 and Section 5), when the UCPW is truncated from below by the North Atlantic Deep Water (NADW) north of 21S, the silica maximum naturally lies at the upper interface between the NADW

and the waters of Antarctic origin. As discussed below, we consider this entire layer to be AAIW north of 21S. The high-nutrient characteristics of the AAIW in the equatorial South Atlantic can be traced northward well into the North Atlantic Ocean (Tsuchiya, 1989; Tsuchiya *et al.,* 1992).

5. Circumpolar Water

The Circumpolar Water (CPW) is a large body of fresh, oxygen-poor, and nutrient-rich water (relative to the NADW) that flows generally eastward in the Antarctic Circumpolar Current and is found over a large density range spanning from $\sim 27.4\ \sigma_\theta$ to $46.06\ \sigma_4$. In the Argentine Basin, the high-oxygen NADW from the north penetrates into the CPW entering from the Drake Passage and divides it into the Upper and Lower Circumpolar Waters (UCPW and LCPW) (Reid *et al.,* 1977; Reid, 1989; Peterson and Whitworth, 1989). As a result, the CPW is characterized by two oxygen minima with the upper minimum (UCPW) sandwiched between the AAIW and the NADW and the lower minimum (LCPW) between the NADW and the oxygen-rich Weddell Sea Deep Water, which is penetrating the Argentine Basin from the Weddell Sea (Section 7).

Stas. 264 and 268 in the Polar Frontal Zone, between the Subantarctic Front (45S) and the Polar Front (49.5S), show remarkable uplifts of the isopleths of all properties. This feature extends from the UCPW through the NADW down to at least 3000 m in the domain of the LCPW and possibly to the bottom at Sta. 264. The feature at Sta. 268 appears to be constrained by the bottom topography (Falkland Ridge). This feature will be discussed in more detail in Section 7.

a. Upper Circumpolar Water. On the present section the upper oxygen minimum associated with the UCPW is clearly evident as a tongue lying below the oxygen maximum of the AAIW and extending from the southern end of the section northward to about 22S. The upper oxygen minimum occurs at $\sigma_\theta = 27.5$–27.7 with a trend toward higher densities in the south. It is shallow (600–800 m) in the north and south and is deepest (1400 m) near 40S. The oxygen content at the minimum is lowest south of 40S and generally increases as far northward as 30S. Farther north it tends to decrease. North of 22S, the intense, shallower equatorial oxygen minimum obliterates the signature of UCPW. The low-oxygen water in the south comes from the South Pacific through Drake Passage (Callahan, 1972; Gordon and Molinelli, 1982, Plates 208 and 226; Peterson and Whitworth, 1989), and that in the north has taken a longer path through the eastern South Atlantic (Reid, 1989, Figs. 18c and 19). The higher-oxygen water in mid-latitudes results from vertical mixing with overlying and underlying waters in the subtropical gyre.

At nearly the same depth as the UCPW oxygen minimum is found a silica maximum, which begins at the Polar Front at 50S and becomes clearly visible north of the Subtropical Front at 41S on the vertical section. It continues as a tongue all the

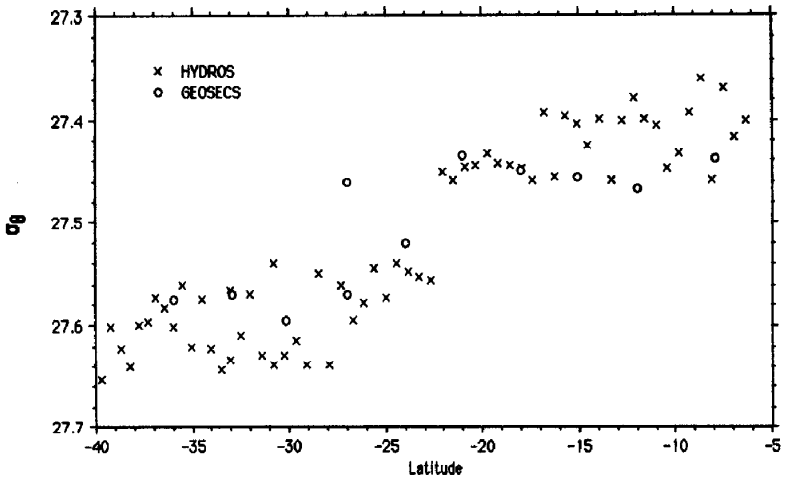

Figure 13. Potential density σ_θ of the silica maximum in the Upper Circumpolar and Antarctic Intermediate Waters along the Hydros 25W section (x) and the GEOSECS western Atlantic section (o).

way to the north end of the section. However, the density at the maximum suddenly shifts at 22S from σ_θ = 27.55–27.65 to σ_θ = 27.35–27.45 (Fig. 13). Mann *et al.* (1973) pointed out a density shift of the silica maximum from σ_θ = 27.6 to 27.4 at 20S on their *Hudson* 70 section along 30W. On the GEOSECS (Geochemical Ocean Sections Study) western Atlantic section (Bainbridge, 1980; 1981), a similar sudden shift can be seen from σ_θ = 27.52 at 24S to σ_θ = 27.43 at 21S. A station at 27S just south of the shift exhibits two maxima of silica at σ_θ = 27.46 and 27.57. The shallower maximum may be a southward extension of the less dense silica maximum observed north of 21S. This sudden density shift indicated by the present and other data and the bifurcation of the silica maximum suggested by the GEOSECS data are the principal bases of the view, expressed in Section 4, that the silica maximum north of 21S belongs to the AAIW and should not be regarded as the northward extension of the silica maximum of the UCPW observed farther south. This latitude of the density shift is almost exactly where the low-oxygen tongue of the UCPW meets the deeper portion of the equatorial oxygen minimum and terminates. It evidently marks the boundary between the anticyclonic subtropical gyre and the cyclonic subequatorial gyre, as already noted for the SAMW and AAIW (Sections 3 and 4).

The UCPW also contains maxima of phosphate and nitrate about 300 m below the upper oxygen minimum. They are found at 27.4–27.6 σ_θ and extend from the south end of the section as far north as 20S. Like the silica maximum, the maxima continue farther north, but shift to lower densities in the range of the AAIW.

Coincident with the silica maximum, a potential-temperature minimum (<2.7°C) extends at ~1600 m depth from the Subtropical Front (41S) to the Brazil Current Front (33S). The potential temperature is highly uniform both vertically and

meridionally in the layer containing this minimum and the underlying maximum, with the temperature difference between the maximum and the minimum being less than 0.1°C. Montgomery (1958) points out that waters with similar characteristics are present in a large amount in the Atlantic between 27S and 45S and in a larger amount in the South Pacific. This uniform layer thus appears to have its origin in the South Pacific.

In the Subantarctic Zone (41–45S), the UCPW also has nearly uniform potential temperature over about 1000 m, but here it is marked by alternating temperature minima and maxima, characteristic of interleaving. On the vertical section, this appears as multiple inversions around 2.6°C. South of the meander or eddy at 45S, which marks the northernmost occurrence of the Subantarctic Front, similar interleaving in a layer of nearly uniform temperature centered around 2.45°C is also found, but the interleaving is not apparent with the contour choice of Figure 2. Farther east at the Greenwich Meridian, no such interleaving appears in the Subantarctic Zone (Whitworth and Nowlin, 1987), but a somewhat thinner (500 m) layer of interleaving is apparent just east of Drake Passage in the Scotia Sea (Peterson and Whitworth, 1989). This interleaving reflects the mechanism by which the CPW becomes saltier and more oxygenated in the South Atlantic (Georgi, 1981a), and it appears to occur primarily in the southwestern South Atlantic in the Subantarctic Zone.

Another potential-temperature minimum, with temperature increasing northward from 3.5°C to 4.4°C, appears near 1000 m north of 21S, of course accompanied by an underlying maximum. The 3.5–4.4°C minimum is distinctly separated along the section from the 2.7°C minimum by a region with no clearly defined minimum. Both Wüst (1935) and Reid (1989) were unable to differentiate between the two temperature minima with their data; Wüst took the northern minimum to be the lower boundary of the AAIW, while Reid treated it as part of the UCPW. The temperature minimum north of 21S is approximately 300 m deeper than the salinity minimum of the AAIW, but is only slightly deeper than the silica maximum. Thus, this northern minimum should be identified with the AAIW.

b. Lower Circumpolar Water. The lower oxygen minimum associated with the LCPW is only weakly expressed at about 3000 m and between 45S (Subantarctic Front) and 41S (Subtropical Front) by the 4.8 ml l^{-1} isopleths in Figure 5. By the individual station data, however, it is more clearly defined and is seen to descend roughly along the 37.06 σ_2 isopycnal from 2000 m at 50S to the bottom (4000 m) near the Tristan da Cunha Fracture Zone (38.5S). Oxygen at the minimum is <4.6 ml l^{-1} at 50S and increases to 4.95 ml l^{-1} at 39S. South of 50S oxygen shows a monotonic increase downward from the upper minimum of the UCPW to the bottom. The LCPW extends beneath the NADW farther north into the Brazil Basin, but here oxygen

decreases monotonically downward with the minimum occurring at the bottom. The bottom water in the Brazil Basin will be discussed in more detail in Section 7.

6. North Atlantic Deep Water

The NADW penetrates into the South Atlantic as a great tongue of saline, oxygen-rich, and nutrient-poor water and can be found at almost all latitudes along the present section. The NADW contains extrema of various properties at different depths, because it does not originate from a single source as is clear from its wide density range and because each property is subject to a boundary condition different from others. Wüst (1935) divided the NADW into three components by using maxima of salinity and oxygen as their identifiers. He designated the mid-depth salinity maximum derived from the Mediterranean outflow water as the Upper North Atlantic Deep Water (UNADW) and the two oxygen maxima found below the salinity maximum as the Middle and Lower North Atlantic Deep Waters (MNADW and LNADW). However, the densities at the extrema change significantly as they extend long distances southward, indicating that a property extremum does not represent the flow path of the same water all along it. Moreover, if we take each of these "waters" to have some thickness above and below the property extremum, the Upper and Middle NADWs must be regarded as largely overlapping, because the salinity maximum and the upper oxygen maximum lie close together. We will refer to the specific property extrema through most of the following.

The first high-resolution measurements of the vertical structure of the NADW were made by Edmond and Anderson (1971) in the Brazil Basin. A recent comprehensive account of the layering of the NADW in terms of property extrema associated with the large-scale circulation in the South Atlantic has been given by Reid (1989).

a. The region north of 25S. North of 25S on the present section, the salinity maximum (UNADW) and the two oxygen maxima (MNADW and LNADW) noted by Wüst (1935) are clearly defined (Fig. 14). The salinity maximum lies at 1700 m near the equator and deepens to 2500 m at 25S. However, most of the deepening occurs between 22S and 25S, where the salinity maximum is truncated by the overlying UCPW at progressively greater depths to the south. North of 21S, a potential-temperature maximum occurs at 1300 m in the layer of sharp vertical salinity gradient just above the salinity maximum. The upper oxygen maximum is about 300 m deeper than the salinity maximum. The deeper oxygen maximum (LNADW) occurs at 3700 m just south of the equator and rises to 3200 m at 25S, where it merges with the upper oxygen maximum (MNADW). The distinction between the two maxima is not clear between 16S and 25S on the vertical section (Fig. 5), but they are distinctly separated by a minimum centered at $\sigma_2 \sim 37.02$ (Fig. 14); the minimum oxygen is about 0.05 ml l^{-1} less than the maxima. The immediate source of this low oxygen

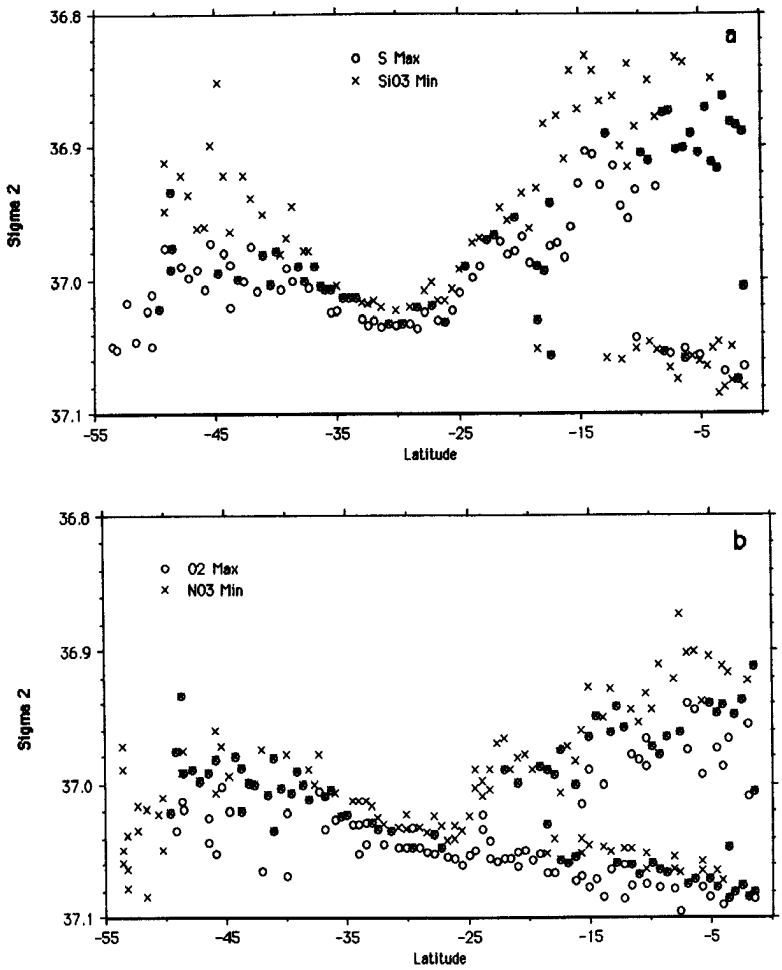

Figure 14. Potential density σ_2 (a) at the salinity maxima and silica minima and (b) at the oxygen maxima and nitrate minima in the North Atlantic Deep Water based on bottle data from the Hydros 25W section.

appears to be the southern or eastern South Atlantic, where CPW-influenced water flows anticyclonically following a path either along the Mid-Atlantic Ridge or across the Ridge from the eastern basin (Fig. 15).

The deeper oxygen maximum (LNADW) is accompanied by nearly vertically-uniform salinity north of 18S. On a small number of stations, notably between 2S and 3°30′S, there is a slight salinity maximum about 250 m above the pronounced oxygen maximum. The salinity maximum is only 0.003 psu higher than the overlying minimum, so is not visible in the contoured vertical sections.

Somewhat above each of the upper and lower maxima of oxygen (MNADW and

Figure 15. Oxygen (ml l^{-1}) on the 37.02 σ_2 isopycnal based on CTD (triangles) and bottle (dots) data. The isopycnal characterizes the North Atlantic Deep Water south of 22S. The shaded region is where the isopycnal shoals to less than 250 m and is associated with the temperature minimum and σ_2 inversions.

LNADW) are found minima of silica, phosphate, and nitrate. Like the layer of nearly uniform salinity associated with LNADW, the deeper minima of the three nutrients are limited to the north of about 18S.

The salinity, oxygen and nutrients at these extrema in the NADW do not change monotonically as they extend southward across the equator. Instead they show a number of isolated cores, which reflect the pattern of the mid-depth zonal circulation. Near the equator, the upper salinity maximum (UNADW) has a core of high salinity (> 34.98 psu) centered at 2S. It is associated with similar cores of high oxygen and low nutrients stretching from the north end of the section to 3–5S. These cores of high salinity, high oxygen, and low nutrients represent an eastward flow of the UNADW and MNADW that are derived from the Mediterranean outflow water and the Labrador Sea Water and that reach the equator in the deep western boundary undercurrent of the North Atlantic (Doney and Bullister, 1992; Tsuchiya *et al.*, 1992). UNADW with salinity higher than 34.98 psu is an eastward extension of the UNADW of this same salinity found all along 37W, including against the western

boundary at this latitude (McCartney, 1993). McCartney showed that this salinity is reduced to 34.96 psu along the western boundary at 11S. This pattern is evident at 36.98 σ_2, slightly below the core of the UNADW, in Reid's (1989) Figure 32b.

The deeper extrema (LNADW) also show cores of high oxygen (>6 ml l^{-1}) and low nutrients just south of the equator. They are pressed against the southern flank of the Mid-Atlantic Ridge. This high-oxygen, low-nutrient water has its origin in the Denmark Strait Overflow Water and also reaches the equator by way of the deep western boundary undercurrent of the North Atlantic (Wüst, 1935; Lynn and Reid, 1968; Tsuchiya *et al.,* 1992). Its North Atlantic source and the eastward near-equatorial spread from the western boundary are clear at 45.86 σ_4 (Reid, 1989, Fig. 36), which characterizes the deep cores near the equator. These waters are also identified in the deep western boundary current immediately south of the equator (McCartney, 1993), in which it is shown that the NADW farther south at 11S is diluted by the strong deep recirculation, compared with the characteristics near the equator and against the Mid-Atlantic Ridge on our section.

At about 10S, properties in the upper salinity maximum of the UNADW (Figs. 3, 5–8) and oxygen at 37.02 σ_2 (Fig. 15) are evidence of another eastward flow from the western boundary. The UNADW core has salinity higher than 34.96 psu, coinciding with cores of high oxygen and low nutrients. The intervening lower-salinity, lower-oxygen water between 6 and 9S suggests westward flow, and hence possibly cyclonic circulation between the equator and 9S.

At about 16S, lateral local minima of salinity and oxygen and lateral local maxima of all three nutrients occur in the entire depth range of the NADW. This pattern is reflected especially well in the map of oxygen at 37.02 σ_2 (Fig. 15). Reid (1989) pointed out that such "breaches" of the NADW are clearly seen near this latitude in Wüst's (1935) vertical sections and in the GEOSECS Atlantic sections (Bainbridge, 1980; Ostlund *et al.,* 1987) and ascribed them to an intrusion of water with a greater CPW component. The water in the breach can be traced back to the Argentine Basin around the eastern end of the eastward-extending core of high salinity and oxygen between 18 and 25S, discussed next. Reid (1989) suggested that it flows northward in the Argentine Basin, turns to the northeast to cross the present section at 30–35S, and then crosses it again at 15–20S after turning back northwestward along the eastern side of an anticyclonic gyre centered north of the Rio Grande Rise (see his Figs. 22–24). The pathlines appear to be in a narrow region above and west of the top of the Mid-Atlantic Ridge, based on data at 30S collected as part of SAVE and used in the map of oxygen at 37.02 σ_2 (Fig. 15).

Just south of the lateral minima of salinity and oxygen, a broad high-salinity core (>34.92 psu) appears at 18–25S. It is associated with a similar core of low silica at about the same density and with cores of high oxygen, low phosphate, and low nitrate at somewhat denser levels. These cores are due to an eastward flow of high-salinity, high-oxygen, low-nutrient water that branches from the southward-flowing deep

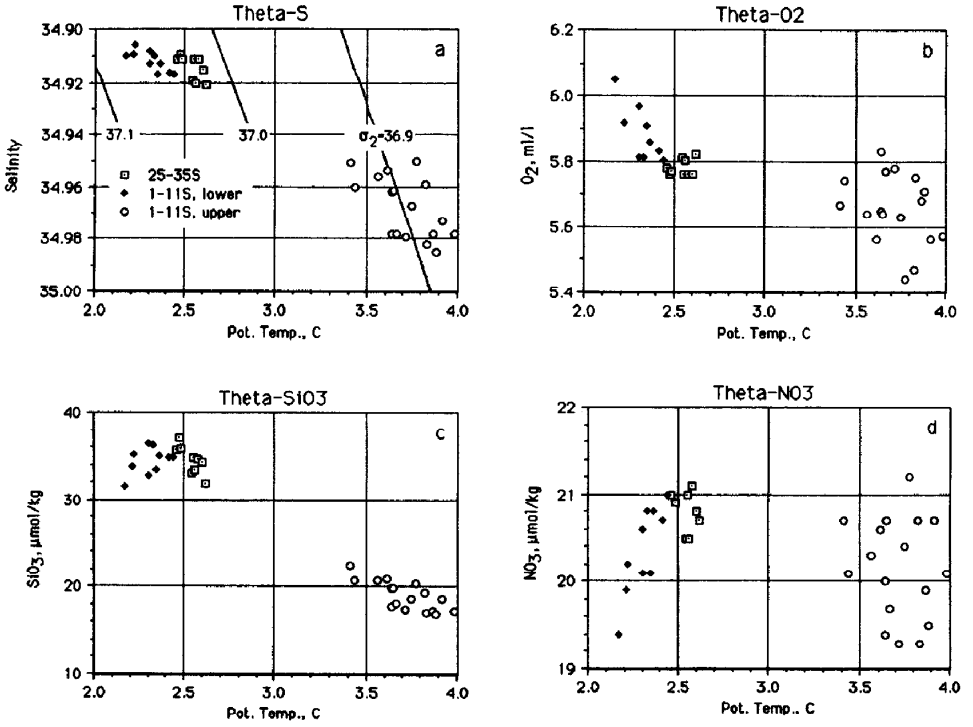

Figure 16. (a) Salinity (psu), (b) oxygen (ml l^{-1}), (c) silica (µmol kg^{-1}), and (d) nitrate (µmol kg^{-1}) at various salinity maxima of the North Atlantic Deep Water plotted against potential temperature (°C). The data are from bottle measurements along the Hydros 25W section. Squares (□) represent the maximum at 25–30S, circles (○) the upper maximum at 1–11S, and solid diamonds (◆) the lower maximum at 1–11S.

western boundary current at 20–25S (Fig. 15; see also Reid, 1989, Figs. 32 and 33). This eastward flow is the southern limb of the anticyclonic gyre mentioned just above.

b. The region south of 25S. South of 25S on our section, the NADW has only a single maximum of salinity and of oxygen and a single minimum of each nutrient, although weak secondary extrema tend to occur south of the Subantarctic Front at 45S. The salinity maximum in this region might appear to be a southward extension of the upper salinity maximum observed north of 11S, and this continuous salinity maximum extending from the North Atlantic was designated UNADW by Wüst (1935). However, inspection of potential temperature versus property diagrams (Fig. 16) reveals that the water characteristics at the salinity maximum south of 25S are considerably different from those at the upper salinity maximum ($\sigma_2 \sim 36.9$) north of 11S, suggesting that these maxima do not belong together. The diagrams also indicate that the characteristics, including potential density, of the maximum south

of 25S are much closer to those at the lower salinity maximum north of 11S. It can be concluded that the southern maximum and the northern lower maximum are derived from the same source waters, whose major component is the Denmark Strait Overflow Water. The less dense portion of the NADW, which contains the upper salinity maximum, is truncated by the UCPW from the south (Section 6a) and simply does not reach the region south of 25S on the present section, although it extends farther south along the western boundary (Reid, 1989, Figs. 21 and 32).

The salinity maximum is at about 3000 m ($\sigma_2 \sim 37.03$) at 30S and rises gradually to 2700 m ($\sigma_2 \sim 36.99$) at 40S. South of 40S, the salinity maximum continues to rise more steeply in unison with the poleward rise of isopycnals in the zone of eastward flow. The salinity maximum is interrupted at the Subtropical Front (42S) and the Subantarctic Front (45S) by lower-salinity water. The density at the maximum exhibits markedly greater scatter in this region (Fig. 14). As elsewhere, the oxygen maximum is slightly deeper (by about 200 m) than the salinity maximum. It rises to a density of 37.02 σ_2 near the Subantarctic Front. The continuous and smooth density modification from the lower oxygen maximum north of 25S to the oxygen maximum south of 25S strongly suggests that the two maxima belong together (Fig. 14b).

The silica minimum is slightly shallower (by only 100 m) than the salinity maximum. Both phosphate and nitrate minima are found at about the same depth as the salinity maximum. The oxygen maximum and the silica minimum terminate at 50S, while the salinity maximum and the phosphate and nitrate minima extend all the way to the southern end of the section.

South of the Brazil Current Front (35S) the lateral gradients of properties at the extrema become more intense than those to the north, indicating the increasingly stronger influence of the CPW. Lateral minima of salinity and oxygen and lateral maxima of all three nutrients are found at Sta. 257 (42°10′S), marking the Subtropical Front Similar lateral extrema of properties at the same latitude are illustrated on the GEOSECS western Atlantic section (Bainbridge, 1980). These lateral extrema are apparently related to an intrusion of the CPW.

In the Subantarctic Zone between the Subtropical Front and Subantarctic Front, the NADW properties are still apparent but with broken and reduced extrema, with salinity between 34.78 and 34.84 psu and oxygen between 4.7 and 5.0 ml l^{-1}. No water with these properties comes through Drake Passage (Sievers and Nowlin, 1984), so it is clearly NADW and not CPW. Whitworth and Nowlin (1987) discuss similar structure at the Greenwich Meridian, where the salinity and oxygen of the NADW north of the Subantarctic Front are similar to what we find at 25–30W in the Subantarctic Zone; they take this to be the mixing of NADW into the CPW, which increases its salinity and oxygen. Peterson and Whitworth (1989) show that the NADW is picked up in the Brazil-Falkland confluence, but it appears that more work might be needed to sort out the full complex of Subantarctic/Subtropical/Brazil Current Fronts in the confluence and hence the exact path of waters of these

properties into the Subantarctic Zone. Waters east of the Brazil Current Front in Peterson and Whitworth have salinity and oxygen higher than 34.9 psu and 5.4 ml l^{-1} and are what we find north of the Brazil Current Front at about 34S.

7. Bottom waters

Relatively cold and fresh bottom waters are found all along the present section and are collectively called the Antarctic Bottom Water (Wüst, 1935). The densest Antarctic water formed in the Weddell Sea (Weddell Sea Bottom Water) remains south of 60S (Reid *et al.,* 1977; Mantyla and Reid, 1983). Using their terminology, we refer to the bottom water south of 41S on this section as Weddell Sea Deep Water (WSDW) and that north of 41S as LCPW (Section 5b).

This identification of WSDW is based on its density. The highest density observed in the Drake Passage is ~46.06 σ_4 so that water denser than this must originate in the Weddell Sea (Sievers and Nowlin, 1984; Reid, 1989). Thus, the 46.06 σ_4 isopycnal can be taken to represent the upper boundary of WSDW. This isopycnal is 2500–4000 m deep in the Georgia and eastern Argentine Basins. In the south it intersects the bottom near the north coast of South Georgia and in the north at 40S.

Because the vertical gradient of density as well as those of temperature and salinity in WSDW is much weaker than in the overlying CPW, it is recognized as a thick layer (~1000 m) of relatively homogeneous bottom water, in which temperature and salinity decrease and oxygen and nutrients generally increase slowly downward. The densest (coldest) WSDW is observed in the Georgia Basin immediately south of the Falkland Ridge (49S). The bottom-water characteristics here are −0.60°C, 34.65 psu, 46.135 σ_4, O_2 ~ 5.6 ml l^{-1}, SiO_3 ~ 124 μmol kg^{-1}, PO_4 ~ 2.2 μmol kg^{-1}, and NO_3 ~ 33 μmol kg^{-1}, right up to the southern flank of the ridge. In the eastern Argentine Basin north of the Falkland Ridge the densest bottom water is −0.25°C, 34.66 psu, 46.09 σ_4, O_2 ~ 5.2 ml l^{-1}, SiO_3 ~ 130 μmol kg^{-1}, PO_4 ~ 2.2 μmol kg^{-1}, and NO_3 ~ 33 μmol kg^{-1}. The differences in properties from the Georgia Basin, where the waters are more purely the coldest WSDW, are as reported in Georgi (1981b) and Whitworth *et al.* (1991).

A notable feature in the Georgia Basin is a weak maximum of silica (> 125 μmol kg^{-1}) 400–800 m above the bottom at Stas. 270–274. Phosphate and nitrate also tend to show weak maxima at about the same depth, but they are not resolved by the isopleths on the vertical sections. The silica maximum occurs at σ_4 ~ 46.10, suggesting that it is a remnant of the silica maximum found at this density in the Weddell Sea (e.g., Carmack, 1973; Gordon and Molinelli, 1982).

The circulation of the eastern Georgia Basin does not appear to be well defined in the literature. WSDW flows into the Argentine Basin from the Weddell Sea along routes both east and west of the Islas Orcadas Rise (Georgi, 1981b; Whitworth *et al.,* 1991). West of the rise, in the Georgia Basin, it flows out to the north through the gap in the Falkland Ridge, at about 36W. Georgi's schematic of the deep circulation

matches the later current-meter observations of Whitworth *et al.* where the latter were available, north of the Falkland Ridge, in the gap, and south of the Falkland Ridge but west of the gap. Georgi shows ambiguous flow direction east of the gap in the Georgia Basin, where our section is located. Both Georgi and Whitworth *et al.* suggest a mid-depth level of no motion, to produce the strong boundary current flows they see. Whitworth *et al.* also show weaker eastward recirculation 100 to 200 km north of the ridge, even though the isopycnal slopes do not change sign, so a single reference level choice would not be appropriate for their data.

On our section, the steep northward descent of the isopycnals at all depths below the surface mixed layer in the Georgia Basin indicates a strong baroclinic shear flow along the southern flank of the Falkland Ridge. Just above the ridge, the isopycnals rise steeply and then fall again north of the ridge. A further steep rise and fall are found at 46S. These slopes are apparent at all depths, and we take them to be associated with the Polar Front in the Georgia Basin, a strong reversed flow just above the Falkland Ridge, and meandering of the Subantarctic Front north of the Falkland ridge. A mid-depth reference level of no motion, based on Whitworth *et al.* (1991), would yield strong westward flow both south and north of the ridge and eastward flow directly above the ridge. Farther from the ridge, choice of a reference level is ambiguous based on Whitworth *et al.*'s measurements. Since our isopycnal slopes north of the Falkland Ridge look very much like their mean isopycnal slopes, we surmise that there is also a weak eastward recirculation north of the boundary current, which is interrupted by the meander at 46S.

The WSDW extends from the Argentine Basin northward into the Brazil Basin through the Vema Channel, but its flow path is confined to the west of 25W (Hogg *et al.*, 1982; Mantyla and Reid, 1983). It does not directly affect our section at 25W, nor does it reach 11S (McCartney and Curry, 1993). Thus, north of 41S on our section the LCPW extends down to the bottom. The maximum density we observed at the crest of the ridge that separates the Argentine and Brazil Basins was 46.00 σ_4.

The LCPW flows northward into the Brazil Basin primarily by way of the Vema Channel (Hogg *et al.*, 1982). There are additional secondary flows through Hunter Channel east of the Rio Grande Rise and on the continental slope west of Vema Channel (Speer *et al.*, 1992). In the Brazil Basin, the boundary between the LCPW and NADW can be defined by a sharp vertical gradient of potential temperature, as well as those of all other properties. At the top of this gradient is a break in the θ-S curve (Wright, 1970; Broecker *et al.*, 1976), which coincides with the deeper oxygen maximum described in Section 6. On our vertical sections the sharp gradients of the properties are seen to be centered at $\sigma_4 \sim 45.92$ (depth $\sim$ 4000 m). Below the high-gradient layer, temperature, salinity, and oxygen decrease and nutrients increase slowly toward the bottom. This thick stratum of vertically homogeneous water is also laterally homogeneous with nearly horizontal isopleths of all properties; there

is no evidence of any singularity in the property fields that suggests strong zonal flow across the 25W section.

The near-bottom water characteristics in the Brazil Basin at 25W are typically 0.19°C, 34.70 psu, 46.045 σ_4, $O_2 \sim 5.15$ ml l^{-1}, $SiO_3 \sim 116$ μmol kg^{-1}, $PO_4 \sim 2.18$ μmol kg^{-1}, and $NO_3 \sim 31$ μmol kg^{-1}. At 11S, the lowest bottom-water temperature is less than 0.1°C and water colder than 0.2°C is limited to west of 28W (McCartney and Curry, 1993). The deeper 0.2°C water found at 25W is derived from this broad western boundary layer.

The near-bottom water at Stas. 318–321 (28–29.5S) in a small trough with a rugged bottom is significantly warmer, saltier, less dense, higher in oxygen, and lower in nutrients than the water at the same depth to the north. This trough may be separated from the main Brazil Basin.

8. Discussion and summary

One of the most significant outcomes of this work is the identification of various fronts in relation to the large-scale circulation and the distribution of mode waters. Five major fronts are identified in the water properties, not all coinciding with strong isopycnal slopes. Those with strong baroclinic shear are the Polar Front at 49°30′S, the Subantarctic Front at 45S, and the Subtropical Front at 41–42S. The Subtropical Front originates between the Brazil and Falkland Current fronts in their confluence (Peterson and Stramma, 1991) and can be considered an extension of the Brazil Current. A second eastward flow, the Brazil Current Front, whose extension to 25W we documented herein, had a weaker baroclinic signature and was located at 34–36S. The boundary between the anticyclonic subtropical and cyclonic subequatorial gyres was marked by a property front at 21S; mid-depth isopycnal slopes change from gently sloping downward toward the south to flat north of the front. The 21S front coincides with the northern terminus of the high-oxygen tongue associated with the Antarctic Intermediate Water and with the abrupt shift in density of the high-silica tongue originating in the Upper Circumpolar Water and extending northward. A weak eastward near-surface flow is indicated at about 25S, marking the southern edge of a mode water, and is probably part of the northern anticyclonic gyre (Tsuchiya, 1985).

Between the Subtropical Front and the Brazil Current Front is found an isopycnal bowl, with intensified westward baroclinic flow at 38–39S. This is likely to be recirculation of the flow in the Subtropical Front. With a bottom reference level of no motion, the eastward transport in the Subtropical Front (Stas. 258–251) is 56 Sv (Sv = 10^6 m^3s^{-1}), and the westward transport in the recirculation (Stas. 251–248) is 12 Sv, for a net eastward flow of 44 Sv. With a 3000 dbar reference level, the eastward transport is 33 Sv, the westward transport is 12 Sv and the net is 21 Sv eastward. The Brazil Current Front transport (Stas. 238–241) is 16 Sv and 14 Sv for a bottom and a 3000 dbar reference level, respectively, with most of the transport in the upper

1000 m. The Subtropical Front therefore is the primary vehicle for the eastward flow from the separated Brazil Current, with a strength equivalent to that at the western boundary; Zemba (1991) calculated a growth of the Brazil Current from 12 Sv at 27S to 80 Sv at 36S, where a compact northward recirculation of about 33 Sv was observed between the Brazil Current and 40W. Our section suggests that part of the recirculation extends well into the central South Atlantic.

Two pycnostads with temperatures 20–24°C (σ_θ = 25.0–25.8) are observed at 10–25S. The southern denser (25.6 σ_θ) one resembles the 18°C Water in the North Atlantic Ocean, but is warmer and located closer to the equator, within the northern subtropical gyre as shown in Tsuchiya (1985). The northern lighter (25.4 σ_θ) pycnostad lies on the south side of the cyclonic subequatorial circulation. Whether they are merely a function of the gyre circulation or have some convective forcing in winter is unclear. Two types of Subantarctic Mode Water are also found, one (centered at 26.7 σ_θ) between the Subtropical Front and the Brazil Current Front, and the other (centered at 26.6 σ_θ) north of the Brazil Current Front. Both are assumed to have convective forcing in winter.

The AAIW forms a weak pycnostad at 4°C between the Subtropical Front and the Subantarctic Front. The characteristics of the pycnostad are similar to those of the densest variety of the SAMW formed by winter convection in the southeastern South Pacific Ocean and the Drake Passage. This finding is consistent with the hypothesis that the densest variety of the SAMW is the source of the AAIW in the southern-hemisphere oceans (McCartney, 1977; 1982).

A subsurface anticyclonic eddy was found in the subtropical gyre at about 28S, containing a type of SAMW which is normally found farther to the southwest and relatively new AAIW. Its maximum geostrophic velocity of 10 cm s^{-1} relative to 1000 dbar appeared at 300 m. It is assumed to have originated in the Brazil Current.

Another important result of this work is the precise description of the structure of the North Atlantic Deep Water, Circumpolar Water, and Weddell Sea Deep Water, made possible by the high quality and high horizontal and vertical resolution of the present data. Our data clearly show that the NADW north of 25S contains two vertical maxima of oxygen separated by intervening low-oxygen water of enhanced circumpolar characteristics. Each oxygen maximum is associated with a maximum of salinity and minima of silica, phosphate, and nitrate. The deeper salinity maximum is only weakly defined. It is limited to the north of 18S as are the deeper minima of the nutrients.

South of 25S only a single maximum of salinity, a single maximum of oxygen, and a single minimum of each nutrient exist in the NADW. Although this salinity maximum is seemingly the southward extension of the shallower salinity maximum north of 25S, the water characteristics of the salinity maximum are more similar to those of the deeper, weaker salinity maximum north of 11S. It is suggested that the maximum south of 25S and the deeper maximum north of 11S are derived from the same source

waters, whose major component is the Denmark Strait Overflow Water. The less dense NADW containing the shallower extrema of characteristics in the north turns to the east at lower latitudes and does not reach the region south of 25S on the 25W section.

The characteristics of the NADW do not change monotonically along this section as it extends southward in the South Atlantic. Instead it exhibits a number of cores interrupted by domains of intensified circumpolar characteristics. This structure of the NADW is found to be closely related to the basin-scale zonal circulation pattern.

The bottom water south of 41S is identified as the WSDW from its high density. It forms a relatively homogeneous layer as thick as 1000 m. The densest WSDW is observed in the Georgia Basin immediately south of the Falkland Ridge. A steep northward descent of isopycnals occurs along the southern flank of the Ridge accompanied by a reversal of the isopycnal slope just above the Ridge. The WSDW that enters the Brazil Basin through the Vema Channel is restricted to the west of 25W so that, on the present section, the Lower Circumpolar Water occupies the bottom layer of the Brazil Basin. Its water characteristics are homogeneous both vertically and meridionally, and there is no evidence that suggests strong zonal flow across the section.

Acknowledgments. This work was supported by the National Science Foundation under Grants OCE86-14486, OCE92-01314, and OCE92-01315. The field work was made possible by the excellent support provided by the Oceanographic Data Facility at Scripps Institution of Oceanography and the captain and crew of R/V *Melville.* Martha Denham assisted with computation. Contribution number 8330 from the Woods Hole Oceanographic Institution.

REFERENCES

Bainbridge, A. E. 1980. GEOSECS Atlantic Expedition, Vol. 2, Sections and profiles. National Science Foundation, Washington, DC, 198 pp.

—— 1981. GEOSECS Atlantic Expedition, Vol. 1, Hydrographic data 1972–1973. National Science Foundation, Washington, DC, 121 pp.

Broecker, W. S., T. Takahashi and Y.-H. Li. 1976. Hydrography of the central Atlantic-I. The two-degree discontinuity. Deep-Sea Res., *23,* 1083–1104.

Brundage, W. L. and J. P. Dugan. 1986. Observations of an anticyclonic eddy of 18°C water in the Sargasso Sea. J. Phys. Oceanogr., *16,* 717–727.

Callahan, J. E. 1972. The structure and circulation of Deep Water in the Antarctic. Deep-Sea Res., *19,* 563–575.

Carmack, E. C. 1973. Silicate and potential temperature in the deep and bottom waters of the western Weddell Sea. Deep-Sea Res., *20,* 927–932.

Doney, S. C. and J. L. Bullister. 1992. A chlorofluorocarbon section in the eastern North Atlantic. Deep-Sea Res., *39,* 1857–1883.

Edmond, J. M. and G. C. Anderson. 1971. On the structure of the North Atlantic Deep Water. Deep-Sea Res., *18,* 127–133.

Georgi, D. T. 1981a. On the relationship between the large-scale property variations and fine structure in the Circumpolar Deep Water. J. Geophys. Res., *86,* 6556–6566.

—— 1981b. Circulation of bottom waters in the southwestern South Atlantic. Deep-Sea Res., *28,* 959–979.

Gordon, A. L. 1981. South Atlantic thermocline ventilation. Deep-Sea Res., *28,* 1239–1264.

Gordon, A. L. and K. T. Bosley. 1991. Cyclonic gyre in the tropical South Atlantic. Deep-Sea Res., *38* (Suppl. 1), S323–S343.

Gordon, A. L. and W. F. Haxby. 1990. Agulhas eddies invade the South Atlantic: evidence from Geosat altimeter and shipboard conductivity-temperature-depth survey. J. Geophys. Res., *95,* 3117–3125.

Gordon, A. L. and E. J. Molinelli. 1982. Thermohaline and chemical distributions and the atlas data set, *in* Southern Ocean Atlas, Columbia University Press, pp. 1–11 and 233 plates.

Gordon, A. L., R. F. Weiss, W. M. Smethie, Jr. and M. J. Warner. 1992. Thermocline and intermediate water communication between the South Atlantic and Indian Oceans. J. Geophys. Res., *97,* 7223–7240.

Hogg, N., P. Biscaye, W. Gardner and W. J. Schmitz, Jr. 1982. On the transport and modification of Antarctic Bottom Water in the Vema Channel. J. Mar. Res., *40* (Suppl.), 231–263.

Lynn, R. J. and J. L. Reid. 1968. Characteristics and circulations of deep and abyssal waters. Deep-Sea Res., *15,* 577–598.

Mann, C. R., A. R. Coote and D. M. Garner. 1973. The meridional distribution of silicate in the western Atlantic Ocean. Deep-Sea Res., *20,* 791–801.

Mantyla, A. W. and J. L. Reid. 1983. Abyssal characteristics of the World Ocean waters. Deep-Sea Res., *30,* 805–833.

McCartney, M. S. 1977. Subantarctic Mode Water, *in* A Voyage of Discovery, George Deacon Anniversary Volume, M. Angel, ed. Pergamon Press, 103–119.

—— 1982. The subtropical recirculation of Mode Waters. J. Mar. Res., *40* (Suppl.), 427–464.

—— 1993. Crossing of the equator by the deep western boundary current in the western Atlantic Ocean. J. Phys. Oceanogr., *23,* 1953–1974.

McCartney, M. S. and R. A. Curry. 1993. Transequatorial flow of Antarctic Bottom Water in the western Atlantic Ocean: abyssal geostrophy at the equator. J. Phys. Oceanogr., *23,* 1264–1276.

McCartney, M. S. and M. E. Woodgate-Jones. 1991. A deep-reaching anticyclonic eddy in the subtropical gyre of the eastern South Atlantic. Deep-Sea Res., *38* (Suppl. 1), S411–S444.

Montgomery, R. B. 1958. Water characteristics of Atlantic Ocean and of world ocean. Deep-Sea Res., *5,* 134–148.

Ostlund, H. G., H. Craig, W. S. Broecker and D. Spencer. 1987. GEOSECS Atlantic, Pacific, and Indian Ocean Expeditions, Vol. 7. Shorebased data and graphics. National Science Foundation, Washington, DC, 200 pp.

Peterson, R. G. and L. Stramma. 1991. Upper-level circulation in the South Atlantic Ocean. Prog. Oceanogr., *26,* 1–73.

Peterson, R. G. and T. Whitworth III. 1989. The Subantarctic and Polar Fronts in relation to the deep water masses through the southwestern Atlantic. J. Geophys. Res., *94,* 10817–10838.

Piola, A. R. and A. L. Gordon. 1989. Intermediate waters in the southwest South Atlantic. Deep-Sea Res., *36,* 1–16.

Reid, J. L. 1989. On the total geostrophic circulation of the South Atlantic Ocean: Flow patterns, tracers, and transports. Prog. Oceanogr., *23,* 149–244.

Reid, J. L., W. D. Nowlin, Jr. and W. C. Patzert. 1977. On the characteristics and circulation of the southwestern Atlantic Ocean. J. Phys. Oceanogr., *7,* 62–91.

Rintoul, S. R. 1991. South Atlantic interbasin exchange. J. Geophys. Res., *96,* 2675–2692.

Roden, G. I. 1986. Thermohaline fronts and baroclinic flow in the Argentine Basin during the austral spring of 1984. J. Geophys. Res., *91,* 5075–5093.

Roden, G. I. 1989. The vertical thermohaline structure in the Argentine Basin. J. Geophys. Res., *94,* 877–896.

Scripps Institution of Oceanography. 1992a. South Atlantic Ventilation Experiment: Chemical, physical and CTD data report, Legs 4, 7 December 1988–15 January 1989, Leg 5, 23 January–8 March 1989, R/V *Melville.* Scripps Institution of Oceanography, University of California, San Diego, SIO Reference *92–10,* 625 pp.

—— 1992b. Hydros Leg 4: Physical, chemical, and CTD data, 13 March–19 April 1989, R/V *Melville.* Scripps Institution of Oceanography, University of California, San Diego, SIO Reference *92–12,* 190 pp.

Sievers, H. A. and W. D. Nowlin, Jr. 1984. The stratification and water masses at Drake Passage. J. Geophys. Res., *89,* 10489–10514.

Speer, K., W. Zenk, G. Siedler, J. Pätzold and C. Heidland. 1992. First resolution of flow through the Hunter Channel in the South Atlantic. Earth Planet. Sci. Lett., *113,* 287–292.

Stramma, L. and R. G. Peterson. 1990. The South Atlantic Current. J. Phys. Oceanogr., *20,* 846–859.

Suga, T. and L. D. Talley. 1994. Antarctic Intermediate Water circulation in the tropical and subtropical South Atlantic. J. Geophys. Res., (submitted).

Tsuchiya, M. 1985. Evidence of a double-cell subtropical gyre in the South Atlantic Ocean. J. Mar. Res., *43,* 57–65.

—— 1989. Circulation of the Antarctic Intermediate Water in the North Atlantic Ocean. J. Mar. Res., *47,* 747–755.

Tsuchiya, M., L. D. Talley and M. S. McCartney. 1992. An eastern Atlantic section from Iceland southward across the equator. Deep-Sea Res., *39,* 1885–1917.

Whitworth, T., III and W. D. Nowlin, Jr. 1987. Water masses and currents of the southern ocean at the Greenwich Meridian. J. Geophys. Res., *92,* 6462–6476.

Whitworth, T., III, W. D. Nowlin, Jr., R. D. Pillsbury, M. I. Moore and R. F. Weiss. 1991. Observations of the Antarctic Circumpolar Current and deep boundary current in the southwest Atlantic. J. Geophys. Res., *96,* 15105–15118.

Wright, W. R. 1970. Northward transport of Antarctic Bottom Water in the western Atlantic Ocean. Deep-Sea Res., *17,* 367–371.

Wüst, G. 1935. Schichtung und Zirkulation des Atlantischen Ozeans. Die Stratosphäre des Atlantischen Ozeans. Wissenschaftliche Ergebnisse der Deutschen Atlantischen Expedition auf dem Forschungs- und Vermessungsschiff "Meteor" 1925–1927, *6* (1),(2), 109–288.

Zemba, J. C. 1991. The structure and transport of the Brazil Current between 27° and 36° South. Ph.D. thesis, Woods Hole Oceanographic Institution/Massachusetts Institute of Technology, 160 pp.

Received: *15 March, 1993;* revised: *2 November, 1993.*